

Algorithms for Ellipsoids

Stephen B. Pope
Sibley School of Mechanical & Aerospace Engineering
Cornell University
Ithaca, New York 14853

Report: FDA-08-01
February 2008

Abstract

We describe a number of algorithms to perform basic geometric operations on ellipsoids in n spatial dimensions, for $n \geq 1$. These algorithms are implemented in `ELL_LIB`, a library of Fortran subroutines. With E , E_1 and E_2 being given ellipsoids, and \mathbf{p} a given point, the tasks considered include: determine the point in E which is closest to \mathbf{p} or furthest from \mathbf{p} ; grow or shrink E so that its boundary intersects \mathbf{p} ; project E onto a given affine space; determine a separating hyperplane between E_1 and E_2 ; determine an ellipsoid (of small volume) which covers E_1 and E_2 .

Contents

1	Introduction	3
2	Representation of ellipsoids	3
3	Summary of routines	5
4	Useful preliminary results	5
4.1	Linear transformation	6
4.2	Quadratic minimization	8
4.3	Householder matrix	8
4.4	Rank-one modification	9
5	Smallest and largest principal semi-axes of E	10
6	Is the point x covered by E?	12
7	Relative distance to the boundary of E	12
8	Nearest point in E to a given point	13
9	Furthest point in E to a given point	14
10	Minimum-volume ellipsoid covering E and p	14
10.1	Householder matrix algorithm	14
10.2	Rank-one modification algorithm	17
10.3	Behavior	17
11	Shrink E based on a given point	18
11.1	Maximum-volume algorithm	19
11.1.1	Algorithm	19
11.1.2	Behavior	19
11.2	Near-content algorithm	20
11.2.1	Algorithm	21
11.2.2	Behavior	22
11.3	Conservative algorithm	22
11.3.1	Algorithm: reduction to 2D	24
11.3.2	Algorithm: solution in 2D	27

12	Orthogonal projection of E onto a given line	29
13	Orthogonal projection of E onto an affine space	30
14	Generate an ellipsoid which does not cover any specified points	32
15	Separating hyperplane of two ellipsoids	34
16	Pair covering query	36
17	Shrink ellipsoid so that it is covered by a concentric ellipsoid	36
18	Ellipsoid that covers two given ellipsoids	38
18.1	Spheroid algorithm	38
18.2	Covariance algorithm	39
18.3	Iterative algorithm	41
18.3.1	Stage 1	41
18.3.2	Stage 2	41
18.3.3	Stage 3	41
18.3.4	Stage 4	42
18.3.5	Stage 5	44
18.3.6	Stage 6	45
18.3.7	Mutual covering	45
18.3.8	Discussion	46
19	Conclusions	46
20	Acknowledgments	46

1 Introduction

In this paper we describe a number of algorithms to perform basic geometric operations on ellipsoids. These algorithms have been implemented in Fortran routines which are contained in the library `ELL_LIB`, which is available at http://eccentric.mae.cornell.edu/~tcg/ELL_LIB.

Ellipsoids arise in numerous computational problems. The algorithms and routines described here have been developed specifically for use in the *in situ* adaptive tabulation (ISAT) algorithm (Pope 1997).

In Sec. 2 we consider different mathematical representations of an ellipsoid E in \mathcal{R}^n , for $n \geq 1$. For $n = 1$, E is a line segment; for $n = 2$, E is an ellipse; for $n = 3$, E is an ellipsoid; and for $n > 3$, E is a hyper-ellipsoid. For simplicity we generally refer to E (for all $n \geq 1$) as an ellipsoid.

A summary of the routines in `ELL_LIB` is provided in Sec. 3. Following some preliminary results in Sec. 4, the algorithms used are described in Secs. 5–18.

2 Representation of ellipsoids

There are many ways to represent ellipsoids, with the different ways arising naturally in different circumstances. In this section we show the relations between the different representations.

Let the ellipsoid E be centered at \mathbf{c} ; let the columns of the $n \times n$ orthogonal matrix \mathbf{U} be unit vectors in the directions of E 's principal axes; and let $\mathbf{\Sigma}$ be the diagonal matrix (with diagonal elements $\Sigma_{ii} = \sigma_i$) such that $1/\sigma_i$ is the length of the i th principal semi-axis. We assume that the principle axes are finite and strictly positive, i.e., $0 < \sigma_i < \infty$. Then E is given by

$$E \equiv \{\mathbf{x} \mid (\mathbf{x} - \mathbf{c})^T \mathbf{U} \mathbf{\Sigma}^2 \mathbf{U}^T (\mathbf{x} - \mathbf{c}) \leq 1\}. \quad (1)$$

This may alternatively be expressed as

$$E \equiv \{\mathbf{x} \mid \|\mathbf{\Sigma} \mathbf{U}^T (\mathbf{x} - \mathbf{c})\| \leq 1\}. \quad (2)$$

or, from the definition $\mathbf{w} \equiv \mathbf{\Sigma} \mathbf{U}^T (\mathbf{x} - \mathbf{c})$,

$$E \equiv \{\mathbf{x} \mid \mathbf{x} = \mathbf{c} + \mathbf{U} \mathbf{\Sigma}^{-1} \mathbf{w}, \|\mathbf{w}\| \leq 1\}. \quad (3)$$

The above three definitions can be re-expressed in terms of different related matrices. Let \mathbf{A} be the matrix

$$\mathbf{A} \equiv \mathbf{U}\mathbf{\Sigma}^2\mathbf{U}^T, \quad (4)$$

appearing in Eq.(1). Evidently \mathbf{A} is symmetric positive definite; its eigenvectors are the columns of \mathbf{U} and its eigenvalues are $\lambda_i = \sigma_i^2$. We denote by $\mathbf{\Lambda} = \mathbf{\Sigma}^2$ the diagonal matrix of eigenvalues. Thus Eqs. (1)–(3) can be trivially re-written by substituting $\mathbf{\Lambda}^{\frac{1}{2}}$ for $\mathbf{\Sigma}$; or less trivially in terms of \mathbf{A} as

$$E \equiv \{\mathbf{x} \mid (\mathbf{x} - \mathbf{c})^T \mathbf{A} (\mathbf{x} - \mathbf{c}) \leq 1\}, \quad (5)$$

$$E \equiv \{\mathbf{x} \mid \|\mathbf{A}^{\frac{1}{2}}(\mathbf{x} - \mathbf{c})\| \leq 1\}, \quad (6)$$

$$E \equiv \{\mathbf{x} \mid \mathbf{x} = \mathbf{c} + \mathbf{A}^{-\frac{1}{2}}\mathbf{w}, \quad \|\mathbf{w}\| \leq 1\}. \quad (7)$$

Let \mathbf{B} be a non-singular square matrix, which we use to form \mathbf{A} as

$$\mathbf{A} = \mathbf{B}\mathbf{B}^T, \quad (8)$$

and let the SVD of \mathbf{B} be

$$\mathbf{B} = \mathbf{U}\mathbf{\Sigma}\mathbf{V}^T. \quad (9)$$

Note that we have from Eq.(9),

$$\mathbf{A} = \mathbf{B}\mathbf{B}^T = \mathbf{U}\mathbf{\Sigma}^2\mathbf{U}^T, \quad (10)$$

consistent with Eq.(4), and showing that there is a family of matrices \mathbf{B} yielding the same matrix \mathbf{A} , namely $\mathbf{B} = \mathbf{U}\mathbf{\Sigma}\mathbf{V}^T$ for given \mathbf{U} and $\mathbf{\Sigma}$ but arbitrary orthogonal \mathbf{V} . In terms of \mathbf{B} , Eqs. (1)–(3) can be reexpressed as

$$E \equiv \{\mathbf{x} \mid (\mathbf{x} - \mathbf{c})^T \mathbf{B}\mathbf{B}^T (\mathbf{x} - \mathbf{c}) \leq 1\}, \quad (11)$$

$$E \equiv \{\mathbf{x} \mid \|\mathbf{B}^T(\mathbf{x} - \mathbf{c})\| \leq 1\}, \quad (12)$$

$$E \equiv \{\mathbf{x} \mid \mathbf{x} = \mathbf{c} + \mathbf{B}^{-T}\mathbf{w}, \quad \|\mathbf{w}\| \leq 1\}, \quad (13)$$

with a different definition of \mathbf{w} .

The matrix \mathbf{B} can also be factored as

$$\mathbf{B} = \mathbf{L}\mathbf{Q}, \quad (14)$$

where \mathbf{L} is lower triangular with positive diagonal elements and \mathbf{Q} is orthogonal. Thus we obtain

$$\mathbf{A} = \mathbf{B}\mathbf{B}^T = \mathbf{L}\mathbf{L}^T, \quad (15)$$

showing that \mathbf{L} is the Cholesky factorization of \mathbf{A} . The definitions of E in terms of \mathbf{B} apply equally in terms of \mathbf{L} , i.e.,

$$E \equiv \{\mathbf{x} \mid (\mathbf{x} - \mathbf{c})^T \mathbf{L}\mathbf{L}^T (\mathbf{x} - \mathbf{c}) \leq 1\}, \quad (16)$$

$$E \equiv \{\mathbf{x} \mid \|\mathbf{L}^T (\mathbf{x} - \mathbf{c})\| \leq 1\}, \quad (17)$$

$$E \equiv \{\mathbf{x} \mid \mathbf{x} = \mathbf{c} + \mathbf{L}^{-T} \mathbf{w}, \|\mathbf{w}\| \leq 1\}. \quad (18)$$

Computationally it is most efficient to use the Cholesky representation of the ellipsoid in terms of \mathbf{c} and \mathbf{L} , and to store \mathbf{L} in packed format. In `ELL_LIB`, routines with names starting `ell_` use this representation, while those with names starting `ellu_` represent \mathbf{L} in unpacked format.

In the algorithms described below, it often happens that an ellipsoid E_1 given by \mathbf{c}_1 and \mathbf{L}_1 is modified to yield an ellipsoid E_2 which is known in terms of \mathbf{c}_2 and \mathbf{B}_2 (i.e., a full matrix). The representation in terms of \mathbf{L}_2 is efficiently and accurately computed by the LQ algorithm. It is stressed that it is much more accurate to obtain \mathbf{L}_2 from the LQ algorithm than from the Cholesky decomposition of $\mathbf{A} = \mathbf{B}_2\mathbf{B}_2^T$. All of the algorithms described below use the LQ algorithms and avoid forming \mathbf{A} .

The following table shows various routines in `ELL_LIB` that can be used to transform between one representation of an ellipsoid and another. In this table, \mathbf{A} denotes the lower triangle of the symmetric matrix \mathbf{A} , while all other symbols have the meanings given above.

3 Summary of routines

Table 2 summarizes the tasks performed by the principal routines in `ELL_LIB`. Here E , E_1 and E_2 denote given ellipsoids, and \mathbf{p} denotes a given point.

4 Useful preliminary results

In this Section we give some general results that are used in the subsequent sections.

Table 1: Routines to transform between different representations

Routine	From	To
ell_bbt2chol	\mathbf{B}	\mathbf{L}
ellu_bbt2chol	\mathbf{B}	\mathbf{L}
ell_bbt2eig	\mathbf{B}	(\mathbf{U}, Σ)
ell_chol2eig	\mathbf{L}	(\mathbf{U}, Σ)
ellu_chol2eig	\mathbf{L}	(\mathbf{U}, Σ)
ell_eig2chol	(\mathbf{U}, Σ)	\mathbf{L}
ell_full2eig	\mathbf{A}	(\mathbf{U}, Σ)
ell_full2low	\mathbf{A}	$\bar{\mathbf{A}}$
ell_low2chol	$\bar{\mathbf{A}}$	\mathbf{L}

4.1 Linear transformation

We consider the linear transformation

$$\mathbf{y} = \mathbf{M}^T(\mathbf{x} - \mathbf{b}), \quad (19)$$

where \mathbf{b} is a specified vector and \mathbf{M} is a specified non-singular $n \times n$ matrix. The inverse transformation is

$$\mathbf{x} = \mathbf{b} + \mathbf{M}^{-T}\mathbf{y}. \quad (20)$$

If the ellipsoid E is defined by

$$E \equiv \{\mathbf{x} \mid \|\mathbf{B}^T(\mathbf{x} - \mathbf{c})\| \leq 1\}, \quad (21)$$

then it is readily shown, from Eq.(20), that it is also given by

$$E = \{\mathbf{y} \mid \|\hat{\mathbf{B}}^T(\mathbf{y} - \hat{\mathbf{c}})\| \leq 1\}, \quad (22)$$

with

$$\hat{\mathbf{B}} \equiv \mathbf{M}^{-1}\mathbf{B}, \quad (23)$$

and

$$\hat{\mathbf{c}} \equiv \mathbf{M}^T(\mathbf{c} - \mathbf{b}). \quad (24)$$

Table 2: Tasks performed by principal routines in ELL LIB

Routine	Section	Task performed
ell_rad_lower	5	Determine the smallest principal semi-axis of E
ell_rad_upper	5	Determine the largest principal semi-axis of E
ellu_rad_upper		
ell_radii_upper	5	Determine the smallest and largest principal semi-axes of E
ellu_radii_upper		
ell_pt_in	6	Determine whether \mathbf{p} is covered by E
ell_pt_dist	7	Determine the relative distance from \mathbf{p} to the boundary of E
ell_pt_near_far	8	Determine the point in E which is nearest to or furthest from \mathbf{p}
ellu_pt_near_far	9	
ell_pt_modify	10.2	Determine E_V , the modification of E of least change of content whose boundary intersects with \mathbf{p}
ell_pt_shrink	11	Shrink E based on \mathbf{p}
ell_pt_hyper	-	Determine a separating hyperplane between E and \mathbf{p}
ell_pts_uncover	14	Determine an ellipsoid (of large content) which does not cover any given point
ell_line_proj	12	Project E onto a given line
ell_aff_pr	13	Project E onto a given affine space
ell_pair_shrink	17	For concentric E_1 and E_2 , shrink E_2 (if necessary) so that it is covered by E_1
ell_pair_separate	15	Determine if E_1 and E_2 intersect; and, if they do not, determine a separating hyperplane
ell_pair_cover_query	16	Determine whether E_1 covers E_2
ell_pair_cover	18	Determine an ellipsoid (of small content) which covers E_1 and E_2

4.2 Quadratic minimization

Several of the algorithms described below depend on the solution to the following problem: determine a vector \mathbf{x} which minimizes the quadratic function

$$g(\mathbf{x}) \equiv \frac{1}{2}\mathbf{x}^T \mathbf{A}\mathbf{x} + \mathbf{b}^T \mathbf{x}, \quad (25)$$

subject to

$$\mathbf{x}^T \mathbf{x} \leq \delta^2, \quad (26)$$

where δ , \mathbf{b} and \mathbf{A} are a given scalar, vector, and symmetric matrix, respectively. Such problems are efficiently solved by the routine `dgqt` from MINPACK-2 (see Averick et al. 1993).

4.3 Householder matrix

Given a vector \mathbf{p} with $p \equiv \|\mathbf{p}\| > 0$, the corresponding Householder matrix $\mathbf{H}(\mathbf{p})$ is defined by

$$\mathbf{H} = \mathbf{I} - 2\mathbf{v}\mathbf{v}^T, \quad (27)$$

where \mathbf{v} is the unit vector

$$\begin{aligned} v_1 &= [(1 + |p_1|)/(2p)]^{\frac{1}{2}}, \\ v_i &= \frac{\text{sign}(p_1)p_i}{2v_1p}, \quad \text{for } i \geq 2. \end{aligned} \quad (28)$$

It is readily shown that \mathbf{H} has the following properties (not all independent):

1. \mathbf{H} is symmetric: $\mathbf{H}^T = \mathbf{H}$.
2. \mathbf{H} is orthogonal: $\mathbf{H}^T \mathbf{H} = \mathbf{I}$.
3. The first column of \mathbf{H} is parallel (or anti-parallel) to \mathbf{p} .
4. All columns of \mathbf{H} except the first are orthogonal to \mathbf{p} .
5. \mathbf{H} maps \mathbf{p} to the first axis: $\mathbf{H}\mathbf{p} = p\mathbf{e}_1$.

Given \mathbf{p} , the routine `ell.house` returns \mathbf{v} .

4.4 Rank-one modification

Let E be an ellipsoid centered at the origin (i.e., $\mathbf{c} = 0$), given in terms of the positive symmetric definite matrix \mathbf{A} , which has SVD $\mathbf{A} = \mathbf{U}\mathbf{\Sigma}^2\mathbf{U}^T$, and Cholesky decomposition $\mathbf{A} = \mathbf{L}\mathbf{L}^T$. For a given vector \mathbf{w} and scalar ρ , let \mathbf{F} be the rank-one modification of \mathbf{A} :

$$\mathbf{F} = \mathbf{A} + \rho\mathbf{w}\mathbf{w}^T. \quad (29)$$

We require \mathbf{F} to be positive symmetric definite, which in turn requires ρ to exceed a critical value ρ_0 ($\rho_0 < 0$) above which all eigenvalues of \mathbf{F} are positive (see item 7 below). Then, the modified ellipsoid E' is defined by

$$E' \equiv \{\mathbf{x} \mid \mathbf{x}^T\mathbf{F}\mathbf{x} \leq 1\}. \quad (30)$$

The following results are readily obtained:

1. For $\rho \geq 0$, $\mathbf{x}^T\mathbf{F}\mathbf{x}$ is greater than or equal to $\mathbf{x}^T\mathbf{A}\mathbf{x}$, and hence E covers E' .
2. For $\rho \leq 0$, $\mathbf{x}^T\mathbf{F}\mathbf{x}$ is less than or equal to $\mathbf{x}^T\mathbf{A}\mathbf{x}$, and hence E' covers E .
3. The eigenvalues of \mathbf{F} are interlaced with those of \mathbf{A} (see Golub and Van Loan 1996, Sec. 8.5.3). Hence the lengths of the principal axes of E and E' are also interlaced.
4. With $\mathbf{z} \equiv \mathbf{\Sigma}\mathbf{U}^T\mathbf{x}$, we have $\mathbf{x}^T\mathbf{A}\mathbf{x} = \mathbf{z}^T\mathbf{z}$, so that E is the unit ball in \mathbf{z} -space. Correspondingly, E' is given by

$$E' = \{\mathbf{z} \mid \mathbf{z}^T(\mathbf{I} + \rho\tilde{\mathbf{w}}\tilde{\mathbf{w}}^T)\mathbf{z} \leq 1\}. \quad (31)$$

where

$$\tilde{\mathbf{w}} = \mathbf{\Sigma}^{-1}\mathbf{U}^T\mathbf{w}. \quad (32)$$

Thus in \mathbf{z} -space, one principal semi-axis of E' is $(1 + \rho|\tilde{\mathbf{w}}|^2)^{-\frac{1}{2}}\tilde{\mathbf{w}}/|\tilde{\mathbf{w}}|$, and the others are orthogonal unit vectors.

5. Similarly, with $\mathbf{y} \equiv \mathbf{L}^T\mathbf{x}$, we have $\mathbf{x}^T\mathbf{A}\mathbf{x} = \mathbf{y}^T\mathbf{y}$, so that E is the unit ball in \mathbf{y} -space. Correspondingly, E' is given by

$$E' = \{\mathbf{y} \mid \mathbf{y}^T(\mathbf{I} + \rho\hat{\mathbf{w}}\hat{\mathbf{w}}^T)\mathbf{y} \leq 1\}. \quad (33)$$

where

$$\hat{\mathbf{w}} = \mathbf{L}^{-1}\mathbf{w}. \quad (34)$$

6. The rank-one modifications to the identity appearing in Eq.(31) has the symmetric square root

$$\mathbf{I} + \rho \tilde{\mathbf{w}} \tilde{\mathbf{w}}^T = \mathbf{G}^2 = (\mathbf{I} + \alpha \tilde{\mathbf{w}} \tilde{\mathbf{w}}^T)(\mathbf{I} + \alpha \tilde{\mathbf{w}} \tilde{\mathbf{w}}^T) \quad (35)$$

where α and ρ are related by

$$\rho = 2\alpha + \alpha^2 |\tilde{\mathbf{w}}|^2, \quad (36)$$

$$\alpha = (\pm\{1 + \rho |\tilde{\mathbf{w}}|^2\}^{\frac{1}{2}} - 1) / |\tilde{\mathbf{w}}|^2. \quad (37)$$

The matrix in Eq.(33) has a similar square root, with the same value of α , since $|\hat{\mathbf{w}}| = |\tilde{\mathbf{w}}|$.

7. The critical value of ρ is

$$\rho_0 = -1 / |\tilde{\mathbf{w}}|^2, \quad (38)$$

corresponding to the smallest value of ρ for which α is real.

5 Smallest and largest principal semi-axes of E

As sketched in Fig. 1, given an ellipsoid E , the task is to determine its smallest and largest principal semi-axes, or equivalently, the radii of the inscribed and circumscribed hyper-spheres, r_{in} and r_{out} , respectively. This task is accomplished by the routines `ell_rad_lower` and `ell_rad_upper`.

Considering the ellipsoid E , Eq.(16), let the SVD of the Cholesky factor \mathbf{L} be

$$\mathbf{L} = \mathbf{U} \mathbf{\Sigma} \mathbf{V}^T, \quad (39)$$

with $\sigma_1 \geq \sigma_2 \geq \dots \geq \sigma_n$ being the components of the diagonal matrix of singular values $\mathbf{\Sigma}$. Then the matrix \mathbf{A} , Eq.(15), is

$$\mathbf{A} = \mathbf{L} \mathbf{L}^T = \mathbf{U} \mathbf{\Sigma}^2 \mathbf{U}^T = \mathbf{U} \mathbf{\Lambda} \mathbf{U}^T. \quad (40)$$

Evidently the columns of \mathbf{U} are eigenvectors of \mathbf{A} , and the diagonal matrix $\mathbf{\Lambda}$ consists of the eigenvalues of \mathbf{A} with components

$$\lambda_i = \sigma_i^2. \quad (41)$$

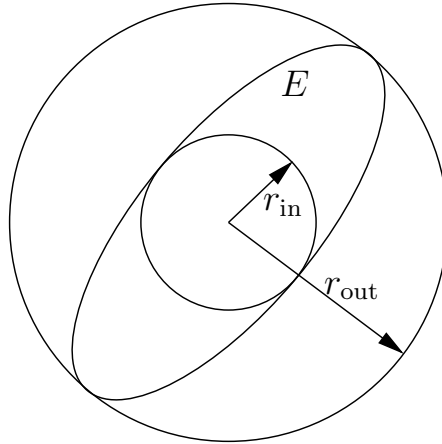


Figure 1: Sketch of an ellipsoid E showing the radii, r_{in} and r_{out} of the inscribed and circumscribed hyper-spheres.

The principal semi-axes are given by $r_i = \lambda_i^{-\frac{1}{2}} = \sigma_i^{-1}$. Thus the smallest principle semi-axis is

$$r_{\text{in}} = [\max(\lambda_i)]^{-\frac{1}{2}}, \quad (42)$$

and the largest is

$$r_{\text{out}} = [\min(\lambda_i)]^{-\frac{1}{2}}. \quad (43)$$

The most stable way to compute r_{in} is as $r_{\text{in}} = 1/\sigma_1$, where σ_1 is obtained from the SVD of \mathbf{L} , and similarly for r_{out} . The routine `ell_radii` determines both r_{in} and r_{out} using the SVD.

The routines `ell_rad_lower` and `ell_rad_upper` determine r_{in} and r_{out} at significantly lower computational cost, but with less accuracy. Given \mathbf{L} , the routine `ell_rad_lower` determines r_{in} via Eq.(42), using the LAPACK routine `dsyevx` to compute the largest eigenvalue of \mathbf{A} .

The routine `ell_rad_upper` determines r_{out} via quadratic minimization. Since r_{out} is the furthest distance from the center to any point on the ellipsoid we have that r_{out}^2 is the maximum of $\mathbf{r}^T \mathbf{r}$ subject to

$$\mathbf{r}^T \mathbf{A} \mathbf{r} \leq 1. \quad (44)$$

By defining $\mathbf{y} = \mathbf{L}^T \mathbf{r}$, this can be put in the standard form of a quadratic minimization problem: $-r_{\text{out}}^2$ is the minimum of

$$-\mathbf{y}^T \mathbf{L}^{-1} \mathbf{L}^{-T} \mathbf{y}, \quad (45)$$

subject to

$$\mathbf{y}^T \mathbf{y} \leq 1. \quad (46)$$

6 Is the point \mathbf{x} covered by E ?

Given a point \mathbf{x} and an ellipsoid E (in terms of \mathbf{c} and \mathbf{L}), the task is to determine whether E covers \mathbf{x} . This is readily determined (by the routine `ell_pt_in`) through the definition of E given by Eq.(17). That is, E covers \mathbf{x} if the quantity

$$s \equiv \|\mathbf{L}^T(\mathbf{x} - \mathbf{c})\|, \quad (47)$$

is less than or equal to unity.

7 Relative distance to the boundary of E

Given an ellipsoid E (in terms of \mathbf{c} and \mathbf{L}) and a point \mathbf{p} ($\mathbf{p} \neq \mathbf{c}$), let \mathbf{b} be the intersection of the ray $\mathbf{c}-\mathbf{p}$ with the boundary of E . The relative distance s to the boundary is defined by:

$$s \equiv |\mathbf{b} - \mathbf{c}|/|\mathbf{p} - \mathbf{c}|. \quad (48)$$

Now the boundary point satisfies

$$\|\mathbf{L}^T(\mathbf{b} - \mathbf{c})\| = 1, \quad (49)$$

and we have

$$\mathbf{b} - \mathbf{c} = s(\mathbf{p} - \mathbf{c}). \quad (50)$$

Hence, s is determined as

$$s = \|\mathbf{L}^T(\mathbf{p} - \mathbf{c})\|^{-1}. \quad (51)$$

The routine `ell_pt_dist` determines s .

It may be noted that the three cases $s < 1$, $s = 1$ and $s > 1$ correspond, respectively, to: \mathbf{p} not being covered by E ; \mathbf{p} being on the boundary of E ; and, \mathbf{p} being covered by E .

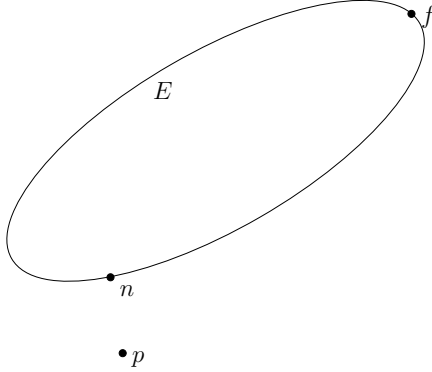


Figure 2: The points n and f in the ellipsoid E which are nearest and furthest, respectively, to the given point p .

8 Nearest point in E to a given point

We consider the ellipsoid E Eq.(16) centered at \mathbf{c} , and a given point \mathbf{p} . The task (performed by the routine `ell_pt_near_far`) is to find the point \mathbf{x} in E closest to \mathbf{p} (see Fig.2). Thus \mathbf{x} satisfies

$$(\mathbf{x} - \mathbf{c})^T \mathbf{L} \mathbf{L}^T (\mathbf{x} - \mathbf{c}) \leq 1, \quad (52)$$

and minimizes

$$s^2 \equiv (\mathbf{x} - \mathbf{p})^T (\mathbf{x} - \mathbf{p}). \quad (53)$$

Evidently, if \mathbf{p} is contained in E then $\mathbf{x} = \mathbf{p}$ and $s = 0$. Otherwise \mathbf{x} is on the boundary of E .

The above equations are readily transformed into the standard quadratic minimization problem. Let \mathbf{y} be defined by

$$\mathbf{y} \equiv \mathbf{L}^T (\mathbf{x} - \mathbf{c}), \quad (54)$$

so that Eq.(52) becomes

$$\mathbf{y}^T \mathbf{y} \leq 1. \quad (55)$$

Equation (54) can be inverted to yield

$$\mathbf{x} = \mathbf{c} + \mathbf{L}^{-T} \mathbf{y}, \quad (56)$$

so that Eq.(53) becomes

$$\begin{aligned} s^2 &= (\mathbf{c} + \mathbf{L}^{-T} \mathbf{y} - \mathbf{p})^T (\mathbf{c} + \mathbf{L}^{-T} \mathbf{y} - \mathbf{p}) \\ &= \mathbf{y}^T \mathbf{L}^{-1} \mathbf{L}^{-T} \mathbf{y} + 2(\mathbf{c} - \mathbf{p})^T \mathbf{y} + (\mathbf{c} - \mathbf{p})^T (\mathbf{c} - \mathbf{p}). \end{aligned} \quad (57)$$

Thus \mathbf{y} is obtained via `dgqt` by minimizing

$$\chi \equiv \frac{1}{2} \mathbf{y}^T \mathbf{L}^{-1} \mathbf{L}^{-T} \mathbf{y} + (\mathbf{c} - \mathbf{p})^T \mathbf{y}, \quad (58)$$

subject to $\|\mathbf{y}\| \leq 1$; and then \mathbf{x} is obtained from Eq.(56).

9 Furthest point in E to a given point

This task is essentially the same as that considered in the previous section, except that the furthest point in E , \mathbf{x} , maximizes $s^2 \equiv \|\mathbf{x} - \mathbf{p}\|^2$, Eq.(53) (rather than minimizing s^2). Thus the same algorithm is used, but the quantity minimized is $-\chi$, Eq.(58) (rather than χ). Again, this is performed by the routine `ell_pt_near_far`.

For all given points \mathbf{p} , the corresponding furthest point \mathbf{x} lies on the boundary of the ellipsoid E (see Fig.2).

10 Minimum-volume ellipsoid covering E and \mathbf{p}

Given an ellipsoid E and a point \mathbf{p} , are seek the ellipsoid E' (concentric with E) of minimum volume which covers both E and \mathbf{p} . In the first subsection we describe an algorithm based on the geometry of the problem. In the subsequent subsection a simpler algorithm is given, which is implemented in the routine `ell_pt_modify`. Then the behavior of the algorithm is examined.

10.1 Householder matrix algorithm

As sketched in Fig. 3(a), consider a given point \mathbf{p} lying outside an ellipsoid E . A modified concentric ellipsoid E' is sought which has minimum volume subject to:

- 1) E' intersects \mathbf{p}
- 2) E' covers E .

This is achieved by

- 1) performing the linear transformation which transforms E to the unit hypersphere, and \mathbf{p} to a point $\hat{\mathbf{p}}$ on the first axis, see Fig. 3 (b)

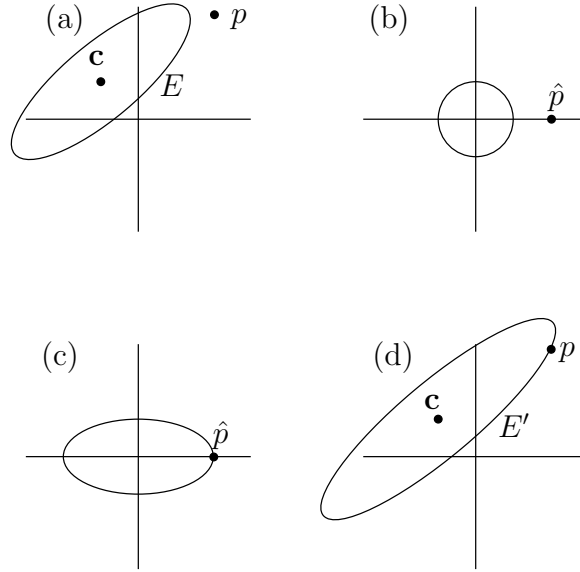


Figure 3: Sketch of: (a) the given ellipsoid E and point p ; (b) the transformation of E to the unit ball, and p to a point on the first axis; (c) the transformed ellipsoid E' ; and (d) the grown ellipsoid E' .

- 2) extending the hypersphere in the first direction to form an ellipsoid with $\hat{\mathbf{p}}$ on its boundary, see Fig. 3 (c)
- 3) inverting the initial transformation to obtain E' , see Fig. 3 (d).

The ellipsoid E (Eq.(17)) is defined by

$$\|\mathbf{L}^T \mathbf{r}\| = \|\mathbf{L}^T(\mathbf{x} - \mathbf{c})\| \leq 1. \quad (59)$$

Defining the transformed variable \mathbf{y} by

$$\mathbf{y} = \mathbf{L}^T(\mathbf{x} - \mathbf{c}), \quad (60)$$

evidently the ellipsoid in \mathbf{y} -space is the unit hypersphere

$$\|\mathbf{y}\| \leq 1. \quad (61)$$

The same transformation applied to \mathbf{p} yield

$$\tilde{\mathbf{p}} = \mathbf{L}^T(\mathbf{p} - \mathbf{c}). \quad (62)$$

There is an orthogonal matrix \mathbf{Q} which transforms $\tilde{\mathbf{p}}$ to a point on the 1-axis; that is,

$$\hat{\mathbf{p}} = \mathbf{Q}^T \tilde{\mathbf{p}} = \mathbf{Q}^T \mathbf{L}^T (\mathbf{p} - \mathbf{c}), \quad (63)$$

where

$$\hat{p}_i = \tilde{p} \delta_{i1}, \quad (64)$$

and $\tilde{p} = \|\tilde{\mathbf{p}}\|$. It is readily shown that \mathbf{Q} is simply the Householder matrix $\mathbf{Q} = \mathbf{H}(\tilde{p})$. The same transformation applied to E yields the unit ball

$$\mathbf{z}^T \mathbf{z} \leq 1, \quad (65)$$

where

$$\mathbf{z} = \mathbf{Q}^T \mathbf{L}^T (\mathbf{x} - \mathbf{c}). \quad (66)$$

This ball and the point $\hat{\mathbf{p}}$ ($\hat{p}_i \equiv \tilde{p} \delta_{i1}$) are shown in Fig. 3 (b). The next step is to define the modified ellipse E' in \mathbf{z} -space, as shown in Fig. 3 (c). This ellipsoid is

$$\mathbf{z}^T \mathbf{\Lambda}^2 \mathbf{z} \leq 1, \quad (67)$$

where

$$\Lambda_{ij}^2 = \delta_{ij} + \delta_{i1} \delta_{j1} (\tilde{p}^{-2} - 1). \quad (68)$$

Transforming back to the original space, we obtain the equation for E' (see Fig. 3 (d)):

$$(\mathbf{x} - \mathbf{c})^T \mathbf{L} \mathbf{Q} \mathbf{\Lambda}^2 \mathbf{Q}^T \mathbf{L}^T (\mathbf{x} - \mathbf{c}) \leq 1, \quad (69)$$

or

$$(\mathbf{x} - \mathbf{c})^T \mathbf{L}' \mathbf{L}'^T (\mathbf{x} - \mathbf{c}) \leq 1. \quad (70)$$

Thus the modified ellipsoid E' has center \mathbf{c} and Cholesky matrix \mathbf{L}' given by

$$\begin{aligned} \mathbf{L}' \mathbf{L}'^T &= \mathbf{L} \mathbf{Q} \mathbf{\Lambda}^2 \mathbf{Q}^T \mathbf{L}^T \\ &= (\mathbf{L} \mathbf{Q} \mathbf{\Lambda}) (\mathbf{L} \mathbf{Q} \mathbf{\Lambda})^T. \end{aligned} \quad (71)$$

In summary, given the ellipsoid E (in terms of \mathbf{c} and \mathbf{L}) and the point \mathbf{p} , then $\tilde{\mathbf{p}}$ is determined by Eq.(62), \mathbf{v} by Eq.(28), \mathbf{Q} by Eq.(27), $\mathbf{\Lambda}^2$ by Eq.(68), and finally the Cholesky matrix of the modified ellipsoid E' is determined by Eq.(71).

10.2 Rank-one modification algorithm

Following from Eqs.(61) and (62), in \mathbf{y} -space, the modified ellipsoid E' is the unit ball extended to intersect the point $\tilde{\mathbf{p}}$. Thus, based on the results of Sec. 4.4, we have

$$E' = \{\mathbf{y} \mid \mathbf{y}^T \mathbf{G}^2 \mathbf{y} \leq 1\}, \quad (72)$$

where

$$\mathbf{G} = \mathbf{I} + \gamma \tilde{\mathbf{p}} \tilde{\mathbf{p}}^T, \quad (73)$$

and γ (determined by the condition $\tilde{\mathbf{p}}^T \mathbf{G}^2 \tilde{\mathbf{p}} = 1$) is

$$\gamma = \left(\frac{1}{|\tilde{\mathbf{p}}|} - 1 \right) \frac{1}{|\tilde{\mathbf{p}}|^2}. \quad (74)$$

Thus, in place of Eq.(71), the Cholesky matrix \mathbf{L}' can be obtained as

$$\mathbf{L}' \mathbf{L}'^T = (\mathbf{L}\mathbf{G})(\mathbf{L}\mathbf{G})^T. \quad (75)$$

This algorithm is implemented in the routine `ell_pt_modify`.

10.3 Behavior

Test are reported for the minimum-volume growing algorithm. The tests are in two dimensions and are based on an initial ellipsoid E (centered at the origin and aligned with the coordinate axes). The length of the major semi-axis is $r_{major} = 1$, and the minor semi-axis is r_{minor} . The grow point \mathbf{p} is not covered by E , and the vector \mathbf{p} is at an angle θ to the x_1 axis. An example of the grown ellipse \tilde{E} given by the minimum-volume algorithm is shown in Fig. 4.

The lengths of the principal semi-axes of the grown ellipse \tilde{E} are denoted by R_{major} and R_{minor} . A figure of demerit F of the growth operation is defined by:

$$F \equiv R_{major} / \max(r_{major}, |\mathbf{p}|) \geq 1. \quad (76)$$

Tests suggest the following behavior:

1. For given E and θ , the maximum of F occurs for $|\mathbf{p}| = r_{major}$, i.e., for \mathbf{p} being on the bounding circle.
2. As illustrated in Fig. 5, for given E , F has a unique maximum (F_{max}) at $\theta = \theta_{max}$ between $\theta = 0$ and $\theta = \pi/2$.

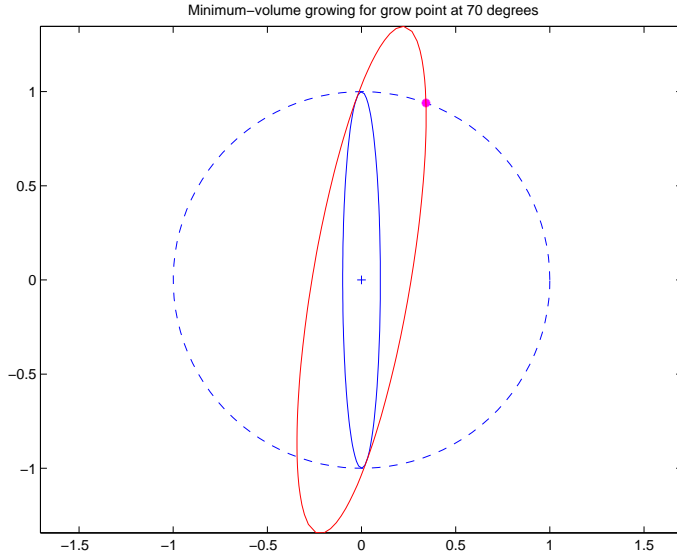


Figure 4: Illustration of the minimum-volume algorithm. The initial ellipse E (solid blue line); its bounding circle (dashed blue line); the grow point \mathbf{p} (magenta); and the grown ellipse (red line) \tilde{E} : $r_{minor} = 0.1$, $|\mathbf{p}| = r_{major} = 1$, $\theta = 70^\circ$.

3. As r_{minor} decreases, θ_{max} tends towards $\pi/2$, and F_{max} tends towards $\sqrt{2}$.

With some justification, it is speculated that even in higher dimensions F is bounded above by $\sqrt{2}$.

11 Shrink E based on a given point

Given an ellipsoid E and a point \mathbf{p} , the problem considered is to generate a concentric ellipsoid E' of smaller volume which covers \mathbf{p} . There is no unique solution to this problem. In the following three subsections we describe three algorithms which yield different solutions for E' , denoted by E_V , E_N and E_C , respectively.

The third (which is based on the first two) is preferred in application to ISAT. The three algorithms are implemented in the routine `ell_pt_shrink` with the parameter `k_ell` set to 1, 2 and 3, respectively.

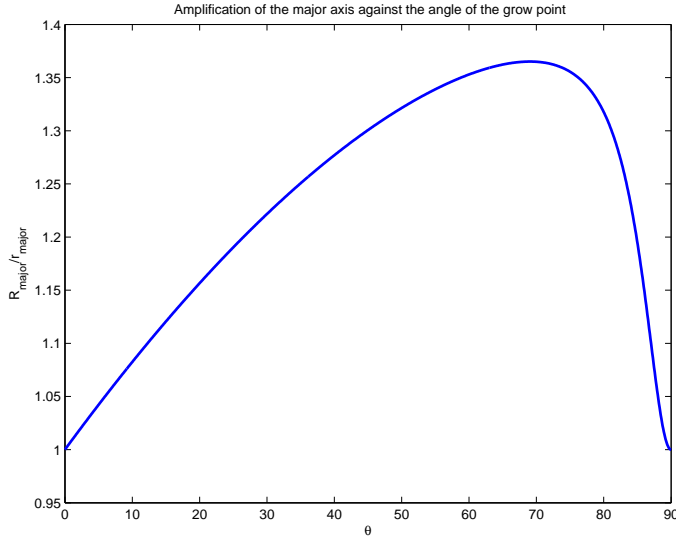


Figure 5: The demerit measure F as a function of the grow-point angle θ : $r_{minor} = 0.1$, $|\mathbf{p}| = r_{major} = 1$.

11.1 Maximum-volume algorithm

11.1.1 Algorithm

The algorithm described in section 10 to grow on ellipsoid E based on a point \mathbf{p} lying outside of E can also be applied when the point \mathbf{p} lies inside E .

The resulting modified ellipsoid E_V has maximal volume subject to:

- 1) \mathbf{p} is on the boundary of E_V
- 2) E_V is covered by E .

11.1.2 Behavior

We consider the same 2D case as for the minimum-volume growing algorithm, except that here the *shrink point* \mathbf{p} is covered by the ellipse E . The maximum-volume shrinking algorithm determines the ellipse E_V of maximum volume which is covered by E and has \mathbf{p} on its boundary. This is illustrated in Fig. 6.

We define a figure of merit

$$F \equiv R_{minor} / \min(r_{minor}, |\mathbf{p}|) \leq 1, \quad (77)$$

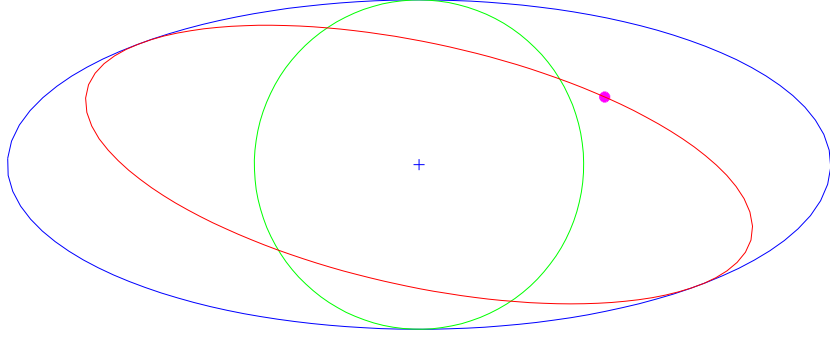


Figure 6: The maximum-volume shrinking algorithm. The initial ellipse E (solid blue line); its inscribed circle (green line); the grow point \mathbf{p} (magenta); and the maximum-volume shrunk ellipse E_V (red line): $r_{minor} = 0.4$, $r_{major} = 1$, $\theta = 70^\circ$, $|\mathbf{p}| = 0.48$.

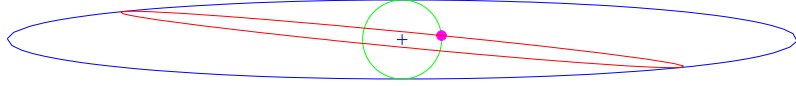


Figure 7: The maximum-volume shrinking algorithm. The initial ellipse E (solid blue line); its inscribed circle (green line); the grow point \mathbf{p} (magenta); and the maximum-volume shrunk ellipse E_V (red line): $r_{minor} = 0.1$, $|\mathbf{p}| = r_{major} = 1$, $\theta = \theta_{min} = 84.3^\circ$.

where r_{minor} and R_{minor} are the lengths of the minor semi-axes before and after shrinking. Based on empirical testing we draw the following conclusions.

1. For given E and θ , the minimum (F_{min}) of F occurs for $\mathbf{p} = r_{minor}$, i.e., for \mathbf{p} lying on the inscribed circle.
2. As r_{minor}/r_{major} decreases, the values of θ at which F is minimum (i.e., $F(\theta_{min}) = F_{min}$) tends to $\pi/2 - r_{minor}/r_{major}$, and F_{min} tends to zero as $2r_{minor}/r_{major}$.

Figure 7 shows the case $r_{minor}/r_{major} = 0.1$, $\theta = \theta_{min} = 84.3^\circ$ for which $F_{min} = 0.1962$.

11.2 Near-content algorithm

As shown above, the maximum-volume shrinking algorithm can lead to very small figures of merit F , Eq.(77). As may be seen from Fig. 7, the shrunk

ellipsoid can exclude a substantial portion of the original ellipsoid which is closer to the center than the shrink point. Here we describe the alternative “near-content shrinking algorithm” which yields values of F of one, or close to one. However, unlike the maximum-volume algorithm, the result depends on the metric of the space. It is implemented in the routine `ell_pt_shrink` (for the parameter value `k_ell= 2`).

11.2.1 Algorithm

We first describe the algorithm and then give its partial justification.

The initial ellipsoid E centered at \mathbf{c} is given in terms of the matrix \mathbf{A} with SVD $\mathbf{A} = \mathbf{U}\Sigma^2\mathbf{U}^T$. We transform to principal axes (\mathbf{y} -space) by defining

$$\mathbf{y} = \mathbf{U}^T \mathbf{x}, \quad (78)$$

and

$$\hat{\mathbf{p}} = \mathbf{U}^T(\mathbf{p} - \mathbf{c}). \quad (79)$$

In \mathbf{y} -space, the modified ellipsoid E_N is defined as the rank-one modification to E :

$$E_N = \{\mathbf{y} \mid \mathbf{y}^T \mathbf{F} \mathbf{y} \leq 1\}, \quad (80)$$

$$\mathbf{F} = \Sigma^2 + \rho \mathbf{w} \mathbf{w}^T, \quad (81)$$

$$\mathbf{w} = \mathbf{D} \hat{\mathbf{p}}, \quad (82)$$

where the diagonal matrix \mathbf{D} is defined by

$$D_{ii} = \max(0, 1/|\hat{\mathbf{p}}|^2 - \Sigma_{ii}^2), \quad (83)$$

and the positive scalar ρ is determined by the intersection condition

$$\hat{\mathbf{p}}^T \mathbf{F} \hat{\mathbf{p}} = 1. \quad (84)$$

We make the following observations about the algorithm:

1. The quantity $1/|\hat{\mathbf{p}}|^2 - \Sigma_{ii}^2$ (appearing in Eq.(83)) is positive if, and only if, the length of the i -th principal semi-axis Σ_{ii}^{-1} is greater than $|\hat{\mathbf{p}}|$.

2. Since E covers $\hat{\mathbf{p}}$, $\hat{\mathbf{p}}^T \mathbf{D} \hat{\mathbf{p}}$ is strictly positive, and hence a positive value of ρ exists which satisfies Eq.(84), namely

$$\rho = (1 - \hat{\mathbf{p}}^T \Sigma^2 \hat{\mathbf{p}}) / (\hat{\mathbf{p}}^T \mathbf{D} \hat{\mathbf{p}}). \quad (85)$$

3. If $\hat{\mathbf{p}}$ lies inside the ball of radius Σ_{11}^{-1} , then $D_{ii} = 1/|\hat{\mathbf{p}}|^2 - \Sigma_{ii}^2$, $\hat{\mathbf{p}}$ is an eigenvector of \mathbf{F} , and hence $\hat{\mathbf{p}}$ is the smallest principal semi-axis of E_N . This is a necessary condition for E_N to be a maximum nearest content ellipsoid.
4. If for some i ($1 \leq i < n$), $\hat{\mathbf{p}}$ lies between the balls of radius Σ_{ii}^{-1} and $\Sigma_{(i+1)(i+1)}^{-1}$, then $w_j = 0$ for $j \leq i$, and as a consequence the first i principal axes of E_N are the same as those of E . This again is a necessary condition for E_N to be a maximum nearest content ellipsoid.

11.2.2 Behavior

The behavior of the near-content algorithm is illustrated for a 2D case in Fig. 8; and it is compared to the maximum-volume algorithm in Fig. 9. There is a striking difference between the two methods, especially for relatively small $|\mathbf{p}|$.

11.3 Conservative algorithm

As may be seen from the last pane in Fig.9, the shrunk ellipsoids (denoted by E_V and E_N) generated by the maximum-volume and near-content algorithms can be quite different. In particular each excludes substantial regions included by the other. Here we describe a third algorithm which is “conservative” in the sense that the shrunk ellipsoid generated, E_C , includes all points in E_V and E_N . Specifically, E_C is defined as the ellipsoid of minimum volume which covers both E_V and E_N . This algorithm is implemented in the routine `ell_pt_shrink` (for the parameter value `k_ell= 3`).

The behavior of the conservative algorithm is illustrated in Fig. 10. It has the following properties:

1. E_C covers \mathbf{p} . Generally, \mathbf{p} is in the interior of E_C .
2. E_C covers both E_V and E_N .
3. In general E_C is not covered by E .

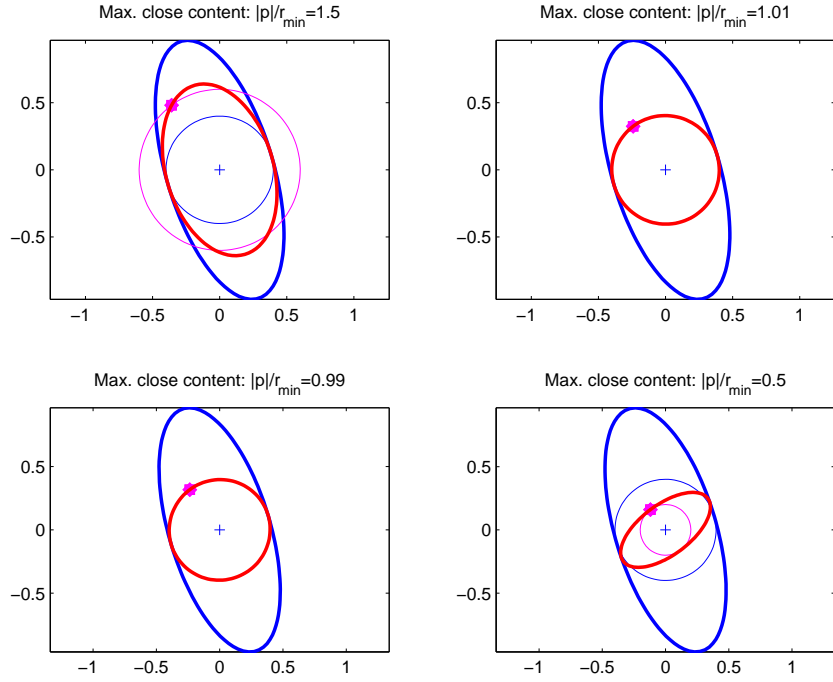


Figure 8: The near-content shrinking algorithm. The initial ellipse E (solid blue line); its inscribed circle (light blue line); the grow point \mathbf{p} (magenta); and the maximum near content shrunk ellipse E_N (red line): $r_{major} = 1$, $r_{minor} = 0.4$, $\theta = 70^\circ$.

4. The largest principal axis of E_C can exceed that of E . Tests suggest that this ratio of principal axes is seldom greater than 1.3.
5. The volume of E_C is no greater than that of E , and in general is less. (This follows from the fact that both E and E_C cover E_V and E_N , but E_C is, by definition, of minimum volume.)
6. If the algorithm is applied a second time to E_C based on the original point \mathbf{p} , the results is (in general) a different ellipsoid. (This is in contrast to the maximum-volume and near-content algorithms in which \mathbf{p} intersects the boundaries of E_V and E_N and hence a re-application of the algorithm has no effect.)
7. Because the algorithm involves E_N , the result E_C depends on the metric of the space.

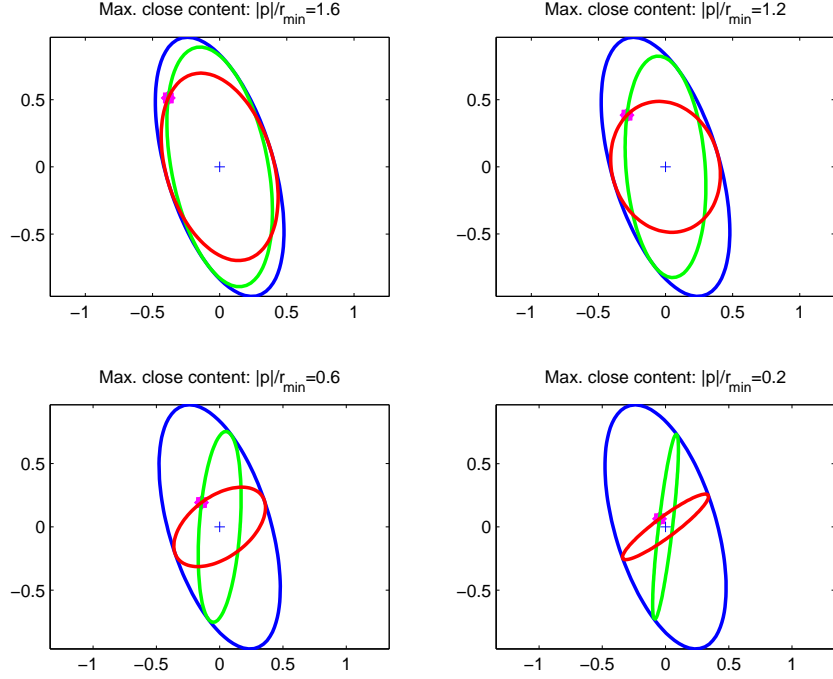


Figure 9: Comparison of the near-content and maximum-volume shrinking algorithms. The initial ellipse E (solid blue line); its inscribed circle (light blue line); the grow point \mathbf{p} (magenta); the near content shrunk ellipse E_N (red line); and the maximum-volume shrunk ellipse E_V (green line): $r_{major} = 1$, $r_{minor} = 0.4$, $\theta = 70^\circ$.

8. Tests reveal that the figure of merit F Eq.(77) is never less than unity.

The algorithm to generate E_C consists of reducing the problem to two dimensions, and then solving a 2D problem. These two parts of the algorithm are described in the following two subsections.

11.3.1 Algorithm: reduction to 2D

Following the development in Sec. 11.2, we transform to the principal axes of E (\mathbf{y} -space), defining \mathbf{y} , $\hat{\mathbf{p}}$ and \mathbf{w} by Eq.(78), Eq.(79) and Eq.(82). Then E_N is defined by

$$E_N = \{\mathbf{y} \mid \mathbf{y}^T \mathbf{F} \mathbf{y} \leq 1\}, \quad (86)$$

with

$$\mathbf{F} = \Sigma^2 + \rho \mathbf{w} \mathbf{w}^T. \quad (87)$$

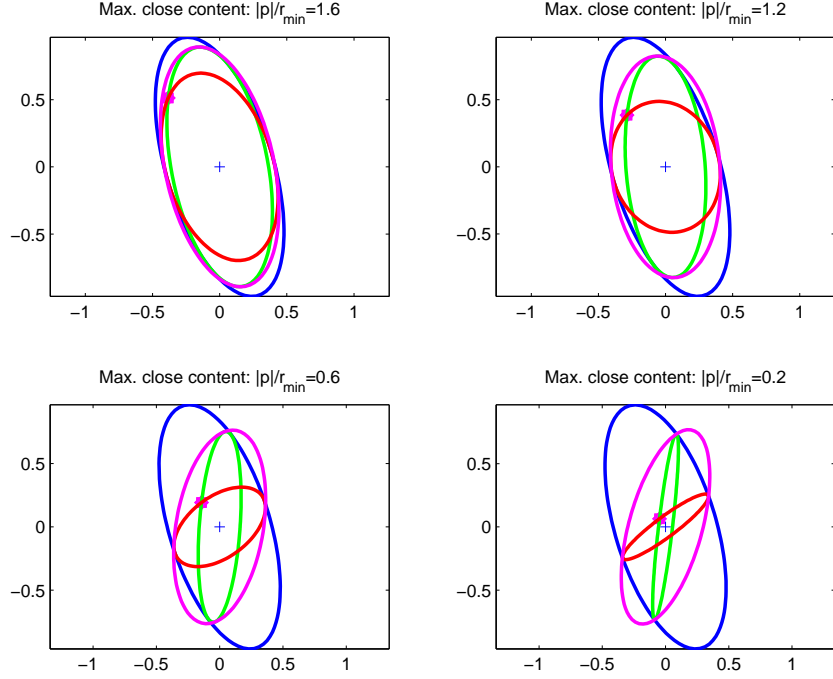


Figure 10: Conservative shrinking algorithm. The initial ellipse E (solid blue line); the grow point \mathbf{p} (magenta); the maximum-volume shrunk ellipse, E_V , (green line); the near-content shrunk ellipse, E_N , (red line); and the conservative shrunk ellipse, E_C , (magenta): $r_{major} = 1$, $r_{minor} = 0.4$, $\theta = 70^\circ$.

We now transform to \mathbf{z} -space in which E is the unit ball:

$$\mathbf{z} = \Sigma \mathbf{y} = \Sigma \mathbf{U}^T \mathbf{x}. \quad (88)$$

In \mathbf{z} -space the definition of E_N , Eq.(86), becomes

$$E_N = \{\mathbf{z} \mid \mathbf{z}^T (\mathbf{I} + \rho \tilde{\mathbf{w}} \tilde{\mathbf{w}}) \mathbf{z} \leq 1\}, \quad (89)$$

with

$$\tilde{\mathbf{w}} = \Sigma^{-1} \mathbf{w}. \quad (90)$$

And the maximum volume shrunk ellipsoid is

$$E_V = \{\mathbf{z} \mid \mathbf{z}^T (\mathbf{I} + \gamma \tilde{\mathbf{p}} \tilde{\mathbf{p}}^T) \mathbf{z} \leq 1\}, \quad (91)$$

where $\tilde{\mathbf{p}}$ is the transform of \mathbf{p}

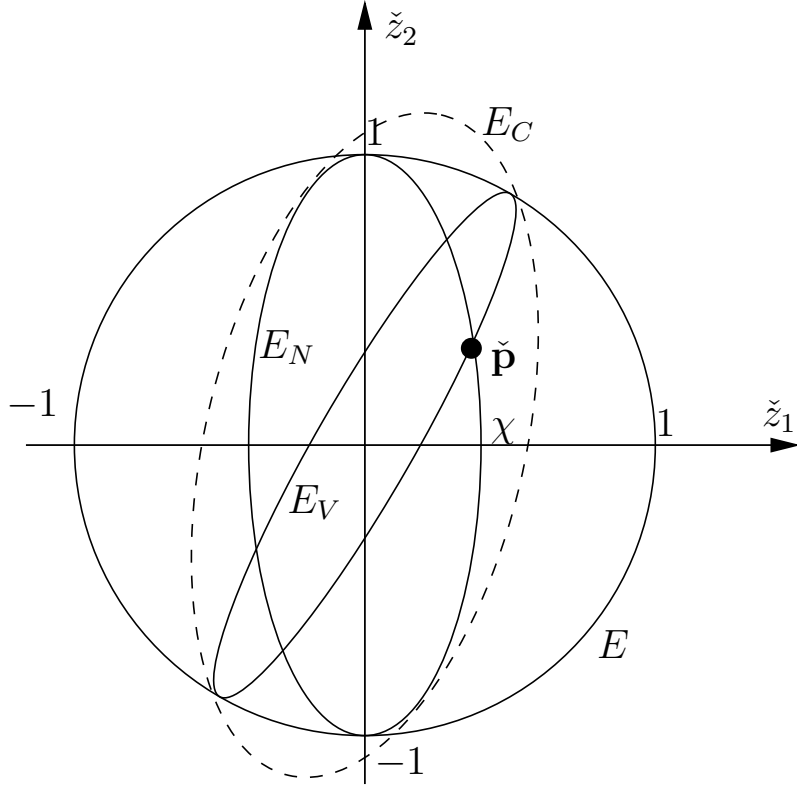


Figure 11: Sketch of E , E_N and E_V in the \check{z}_1 - \check{z}_2 plane (in which E is the unit disc) and of E_C which covers E_N and E_V . The boundaries of both E_N and E_V intersect the grow point $\check{\mathbf{p}}$.

$$\check{\mathbf{p}} = \Sigma \hat{\mathbf{p}} = \Sigma \mathbf{U}^T (\mathbf{p} - \mathbf{c}), \quad (92)$$

(see Eq.(72)). The scalars ρ and γ are determined by the condition that the boundaries of E_N and E_V intersect $\check{\mathbf{p}}$ (in \mathbf{z} -space).

Note that E_N and E_V are completely determined by two vectors, $\tilde{\mathbf{w}}$ and $\tilde{\mathbf{p}}$. If these are co-linear, then $E_N = E_V = E_C$. Otherwise we perform a rotation

$$\check{\mathbf{z}} = \mathbf{Q}^T \mathbf{z}, \quad \check{\mathbf{w}} = \mathbf{Q}^T \tilde{\mathbf{w}}, \quad \check{\mathbf{p}} = \mathbf{Q}^T \tilde{\mathbf{p}}, \quad (93)$$

such that $\check{\mathbf{w}}$ is in the \check{z}_1 -direction, and $\check{\mathbf{p}}$ is in the \check{z}_1 - \check{z}_2 plane. The appropriate orthogonal matrix \mathbf{Q} is obtained from the QR decomposition

$$\mathbf{QR} = [\check{\mathbf{w}} \ \check{\mathbf{p}}]. \quad (94)$$

Figure 11 is a sketch of the intersection of the ellipsoids with the \check{z}_1 - \check{z}_2 plane. Note that in the other directions the principal semi-axes are unit vectors aligned with the coordinate axes. The minimum volume ellipsoid E_C covering E_N and E_V is also shown in the figure. Its intersection with the \check{z}_1 - \check{z}_2 plane is given by the ellipse

$$E'_C = \{(\check{z}_1, \check{z}_2) \mid \|\bar{\mathbf{L}}^T \begin{bmatrix} \check{z}_1 \\ \check{z}_2 \end{bmatrix}\| \leq 1\}, \quad (95)$$

where $\bar{\mathbf{L}}$ is a 2×2 Cholesky matrix which is determined in the next subsection. Thus the ellipsoid E_C is given by

$$E_C = \{\check{\mathbf{z}} \mid \|\check{\mathbf{L}}^T \check{\mathbf{z}}\| \leq 1\}, \quad (96)$$

where the $n \times n$ Cholesky matrix $\check{\mathbf{L}}$ is

$$\check{\mathbf{L}} = \begin{bmatrix} \bar{\mathbf{L}} & \mathbf{0} \\ \mathbf{0} & \mathbf{I} \end{bmatrix}. \quad (97)$$

Transforming Eq.(96) back to the original \mathbf{x} -space, we obtain

$$E_C = \{\mathbf{x} \mid \|\mathbf{L}_C^T(\mathbf{x} - \mathbf{c})\| \leq 1\}, \quad (98)$$

where the Cholesky matrix \mathbf{L}_C is obtained from

$$\mathbf{A}_C = \mathbf{L}_C \mathbf{L}_C^T = \mathbf{B}_C \mathbf{B}_C^T, \quad (99)$$

$$\mathbf{B}_C = \mathbf{U} \Sigma \mathbf{Q} \check{\mathbf{L}}. \quad (100)$$

11.3.2 Algorithm: solution in 2D

The problem to be solved is the determination of the 2×2 Cholesky matrix $\bar{\mathbf{L}}$ defining the covering ellipse E_C in the \check{z}_1 - \check{z}_2 plane (see Fig. 11).

The scalars ρ and γ in Eq.(89) and Eq.(91) are determined by the intersection condition (of ∂E_N and ∂E_V with $\check{\mathbf{p}}$) to be

$$\rho = (1 - |\check{\mathbf{p}}|^2)/\check{p}_1^2, \quad (101)$$

$$\gamma = (1 - \check{\mathbf{p}}^2)/|\check{\mathbf{p}}|^4, \quad (102)$$

and the intersection of E_N with the \check{z}_1 axis is at $\check{z}_1 = \chi$

$$\chi = \frac{|\check{p}_1|}{\sqrt{1 - \check{p}_2^2}}. \quad (103)$$

A transformation to ζ -space is performed

$$\begin{bmatrix} \zeta_1 \\ \zeta_2 \end{bmatrix} = \mathbf{C} \begin{bmatrix} \check{z}_1 \\ \check{z}_2 \end{bmatrix} = \begin{bmatrix} 1/\chi & 0 \\ 0 & 1 \end{bmatrix} \begin{bmatrix} \check{z}_1 \\ \check{z}_2 \end{bmatrix}, \quad (104)$$

consisting of a stretching in the \check{z}_1 direction so that E_N transforms to the unit disc.

With this transformation E_V becomes

$$E_V = \{\zeta \mid \zeta^T \widetilde{\mathbf{A}} \zeta \leq 1\}, \quad (105)$$

with

$$\widetilde{\mathbf{A}} = \begin{bmatrix} a & c \\ c & b \end{bmatrix} = \begin{bmatrix} \chi^2(1 + \gamma\check{p}_1^2) & \gamma\chi\check{p}_1\check{p}_2 \\ \gamma\chi\check{p}_1\check{p}_2 & 1 + \gamma\check{p}_2^2 \end{bmatrix}. \quad (106)$$

The SVD of $\widetilde{\mathbf{A}}$ is

$$\widetilde{\mathbf{A}} = \widetilde{\mathbf{U}} \widetilde{\Sigma}^2 \widetilde{\mathbf{U}}^T, \quad (107)$$

with

$$\widetilde{\mathbf{U}} = \begin{bmatrix} \cos \theta & \sin \theta \\ -\sin \theta & \cos \theta \end{bmatrix}, \quad (108)$$

$$\theta = \frac{1}{2} \tan^{-1}(-2c/(a - b)), \quad (109)$$

$$\widetilde{\Sigma}_{11}^2 = a \cos^2 \theta - 2c \sin \theta \cos \theta + b \sin^2 \theta, \quad (110)$$

$$\widetilde{\Sigma}_{22}^2 = a \sin^2 \theta + 2c \sin \theta \cos \theta + b \cos^2 \theta. \quad (111)$$

Now E_C is the ellipse which covers E_N (which is the unit disc) and E_V which has principal semi-axes whose directions are given by the columns of $\widetilde{\mathbf{U}}$ and whose lengths are $\widetilde{\Sigma}_{11}^{-1}$ and $\widetilde{\Sigma}_{22}^{-1}$. (In general, one of $\widetilde{\Sigma}_{11}$ and $\widetilde{\Sigma}_{22}$ is less than unity and one greater than unity.) Thus the covering ellipse E_C has the same principal directions

$$E_C = \{\zeta \mid \zeta^T \widetilde{\mathbf{U}} \widehat{\Sigma}^2 \widetilde{\mathbf{U}}^T \zeta \leq 1\}, \quad (112)$$

and eigenvalues

$$\widehat{\Sigma}_{11} = \min(1, \widetilde{\Sigma}_{11}), \quad (113)$$

$$\widehat{\Sigma}_{22} = \min(1, \widetilde{\Sigma}_{22}). \quad (114)$$

Transforming back to \check{z}_1 - \check{z}_2 we obtain the required result that E_C is given by Eq.(95), where the 2×2 Cholesky matrix $\bar{\mathbf{L}}$ is obtained as

$$\bar{\mathbf{L}} \bar{\mathbf{L}}^T = \mathbf{C} \widetilde{\mathbf{U}} \widehat{\Sigma}^2 \widetilde{\mathbf{U}}^T \mathbf{C}. \quad (115)$$

12 Orthogonal projection of E onto a given line

We consider a given line \mathcal{L} , parameterized by s , defined by

$$\mathcal{L} \equiv \{\mathbf{x} \mid \mathbf{x} = \mathbf{x}_0 + s\mathbf{v}\}, \quad (116)$$

where \mathbf{x}_0 is a given point and \mathbf{v} is a given non-zero vector, see Fig. 12. Given any point \mathbf{x} in the space, its orthogonal projection onto \mathcal{L} corresponds to

$$s = \frac{\mathbf{v}^T(\mathbf{x} - \mathbf{x}_0)}{\mathbf{v}^T \mathbf{v}}. \quad (117)$$

Now the given ellipsoid E is given by

$$E = \{\mathbf{x} \mid \mathbf{x} = \mathbf{c} + \mathbf{L}^{-T} \mathbf{y}, \|\mathbf{y}\| \leq 1\}. \quad (118)$$

Thus the projection of points in E correspond to values of s

$$\begin{aligned} s &= \frac{\mathbf{v}^T(\mathbf{L}^{-T} \mathbf{y} + \mathbf{c} - \mathbf{x}_0)}{\mathbf{v}^T \mathbf{v}} \\ &= \mathbf{s}_0 + \mathbf{w}^T \mathbf{y}, \quad \text{for } \|\mathbf{y}\| \leq 1, \end{aligned} \quad (119)$$

where

$$\mathbf{s}_0 \equiv \frac{\mathbf{v}^T(\mathbf{c} - \mathbf{x}_0)}{\mathbf{v}^T \mathbf{v}}, \quad (120)$$

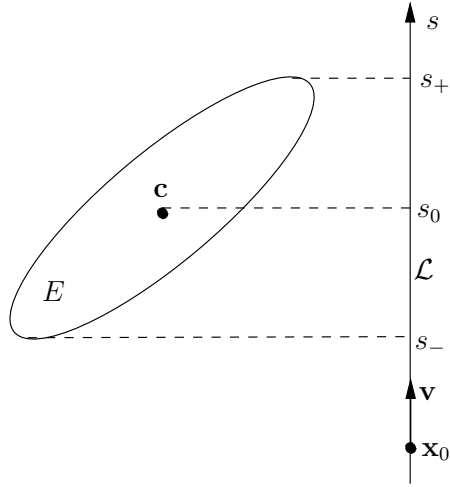


Figure 12: The orthogonal projection of the ellipsoid E onto the line \mathcal{L} is the interval $[s_-, s_+]$.

and

$$\mathbf{w} \equiv \frac{\mathbf{L}^{-1}\mathbf{v}}{\mathbf{v}^T\mathbf{v}}. \quad (121)$$

Given the condition $\|\mathbf{y}\| \leq 1$, it is evident from Eq.(119) that the orthogonal projection of E onto \mathcal{L} corresponds to the interval $[s_-, s_+]$ in s , with

$$s_{\pm} \equiv s_0 \pm |\mathbf{w}|. \quad (122)$$

This is sketched in Fig. 12. This method is implemented in the routine `ell_line_proj`.

13 Orthogonal projection of E onto an affine space

We consider an ellipsoid E (in \mathfrak{R}^n), an affine space A (in \mathfrak{R}^m), for $1 \leq m \leq n$, and the orthogonal projection $P(E)$ of E onto A .

The ellipsoid E is given by

$$E \equiv \{\mathbf{x} \mid \mathbf{x} = \mathbf{c} + \mathbf{L}^{-T}\mathbf{u}, \|\mathbf{u}\| \leq 1\}. \quad (123)$$

The affine space A is given by

$$A \equiv \{\mathbf{x} \mid \mathbf{x} = \mathbf{d} + \mathbf{T}\mathbf{t}\}, \quad (124)$$

where \mathbf{d} is a given m -vector, \mathbf{T} is a given $n \times m$ orthogonal matrix, and \mathbf{t} is a vector of m parameters. The orthogonal projection of a general point \mathbf{x} onto A is

$$P(\mathbf{x}) = \mathbf{d} + \mathbf{T}\mathbf{T}^T(\mathbf{x} - \mathbf{d}). \quad (125)$$

We thus obtain

$$P(E) = \{\mathbf{x} \mid \mathbf{x} = \mathbf{d} + \mathbf{T}\mathbf{T}^T(\mathbf{c} - \mathbf{d} + \mathbf{L}^{-T}\mathbf{u}), \|\mathbf{u}\| \leq 1\}. \quad (126)$$

Now let the SVD of $\mathbf{T}^T\mathbf{L}^{-T}$ be

$$\mathbf{T}^T\mathbf{L}^{-T} = \mathbf{U}[\mathbf{\Sigma} \mathbf{0}]\mathbf{V}^T. \quad (127)$$

Then

$$\mathbf{T}^T\mathbf{L}^{-T}\mathbf{u} = \mathbf{U}\mathbf{\Sigma}\tilde{\mathbf{w}}, \quad (128)$$

where $\tilde{\mathbf{w}}$ denotes the first m elements of

$$\mathbf{w} \equiv \mathbf{V}^T\mathbf{u}. \quad (129)$$

Note that $\|\mathbf{u}\| \leq 1$ implies $\|\tilde{\mathbf{w}}\| \leq 1$. Thus we obtain

$$P(E) = \{\mathbf{x} \mid \mathbf{x} = \mathbf{d} + \mathbf{T}(\tilde{\mathbf{c}} + \mathbf{U}\mathbf{\Sigma}\tilde{\mathbf{w}}), \|\tilde{\mathbf{w}}\| \leq 1\}, \quad (130)$$

where

$$\tilde{\mathbf{c}} \equiv \mathbf{T}^T(\mathbf{c} - \mathbf{d}). \quad (131)$$

The above equation for $P(E)$ is for an m -dimensional ellipsoid in A . It can be put in standard form by defining \mathbf{B} by

$$\mathbf{B}^{-T} = \mathbf{U}\mathbf{\Sigma}, \quad (132)$$

and then $\tilde{\mathbf{L}}$ as

$$\tilde{\mathbf{L}}\tilde{\mathbf{L}}^T = \mathbf{B}\mathbf{B}^T, \quad (133)$$

so that we can write

$$P(E) = \{\mathbf{x} \mid \mathbf{x} = \mathbf{d} + \mathbf{T}(\tilde{\mathbf{c}} + \tilde{\mathbf{L}}^{-T}\tilde{\mathbf{w}}), \|\tilde{\mathbf{w}}\| \leq 1\}. \quad (134)$$

The Cholesky matrix $\tilde{\mathbf{L}}$ can be computed from the LQ decomposition

$$\mathbf{U}\mathbf{\Sigma}^{-1} = \tilde{\mathbf{L}}\mathbf{Q}. \quad (135)$$

This method is implemented in the routine `ell_aff_pr`.

14 Generate an ellipsoid which does not cover any specified points

We are given a point \mathbf{c} , a set of P points $\mathbf{p}^{(j)}(j = 1 : P)$ and a positive length r_{\max} . The problem is to generate an ellipsoid E which

1. is centered at \mathbf{c}
2. has principal semi-axes no larger than r_{\max}
3. does not cover any of the P points
4. and is “as large as possible” (in an undefined sense).

The algorithm used to solve this problem is implemented in the routine `ell_pts_uncover`. It involves a user-specified parameter θ ($0 < \theta \leq 1$) which affects the shape of the resulting ellipsoid, E .

The algorithm has two phases. In the first phase there are n stages which generate a succession of ellipsoids E_1, E_2, \dots, E_n . In the second phase, E is formed by shrinking E_n uniformly and minimally so that none of the points is covered.

In the first phase, a principle axis is determined on each stage. The ellipsoid E_k is determined on the k th stage, and it has the following properties:

1. E_k is centered at \mathbf{c}
2. for $1 \leq \ell < k$, the ℓ th principle axis of E_k is the same as that of E_ℓ (previously determined on stage ℓ)
3. the k th principle axis (of half-length $r_k \leq r_{\max}$) is determined on the k th stage
4. for $k < \ell \leq n$, the ℓ th principle axis of E_k is of half-length r_k .

Note that E_1 is a ball of radius r_1 .

An orthonormal basis is developed with basis vectors $\mathbf{e}_1, \mathbf{e}_2, \dots, \mathbf{e}_n$. On the k th stage \mathbf{e}_ℓ ($\ell \geq k$) is modified, but subsequently \mathbf{e}_k is not altered. At the end of the k th stage, the basis vectors are principal axes of E_k . The vectors $\mathbf{y}^{(j)}(j = 1 : P)$ store the coordinates of the points (relative to \mathbf{c}) in the current basis. For the j th particle we define

$$h_j = \sum_{i=1}^n (y_i^{(j)}/r_i)^2. \quad (136)$$

At the end of the k th stage (since $r_\ell = r_k$ for $\ell \geq k$) we can decompose h_j as

$$h_j = f_j + g_j/r_k^2, \quad (137)$$

where

$$f_j = \sum_{i=1}^{k-1} (y_i^{(j)}/r_i)^2, \quad (138)$$

and

$$g_j = \sum_{i=1}^n (y_i^{(j)})^2. \quad (139)$$

The ellipsoid E_k does not cover the point j if h_j is greater than unity. This condition ($h_j > 1$) can be re-expressed as

$$g_j/r_k^2 > (1 - f_j). \quad (140)$$

Points with $f_j > 1$ cannot be covered by E_k regardless of how large r_k is. Such points are “excluded.” Points with

$$\theta^2 < f_j \leq 1, \quad (141)$$

are “partially excluded.” Such points cannot be covered by E_k shrunk by a factor of θ . The remaining points (i.e., with $f_j \leq \theta^2$) are “included.”

We define \hat{r}_k^2 to be the minimum value over the included points of $g_j/(1 - f_j)$, and denote by \hat{j} the index of a point that achieves this minimum. The significance of \hat{r}_k is that if r_k is set to \hat{r}_k , then the point \hat{j} is on the boundary of E_k , but no points are in the interior of E_k . If \hat{r}_k is greater than r_{max} (or if there are no included points), then we get $r_\ell = r_{max}$ for all $\ell \geq k$, and omit the remaining stages of the first phase. Otherwise r_k is set to \hat{r}_k , and the basis vectors \mathbf{e}_ℓ ($k \leq \ell \leq n$) are re-defined so that $y_\ell^{(\hat{j})} = 0$ for $\ell > k$. In this way, in subsequent stages, the ellipsoid can expand in directions orthogonal to $\mathbf{y}^{(\hat{j})}$, with $\mathbf{y}^{(\hat{j})}$ remaining on the boundary.

At the end of the first phase there are no included points, and E_n does not cover any excluded points. However E_n may cover one or more partially excluded points. Consequently, the final result E is obtained by shrinking E_n uniformly, as little as possible so that none of the partially included points is covered.

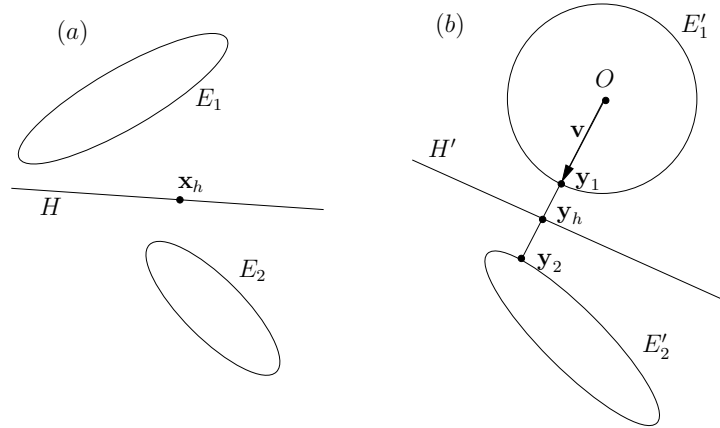


Figure 13: (a) Sketch of the non-intersecting ellipsoids E_1 and E_2 and a separating hyperplane H (b) Corresponding sketch in the transformed space in which E'_1 is the unit ball.

15 Separating hyperplane of two ellipsoids

Given two ellipsoids, E_1 and E_2 , the task is to determine if they intersect; and, if they do not intersect, to determine a separating hyperplane, H . This is performed by the routine `ell_pair_separate`.

The ellipsoid E_1 is given by

$$E_1 \equiv \{\mathbf{x} \mid \|\mathbf{L}_1^T(\mathbf{x} - \mathbf{c}_1)\| \leq 1\}, \quad (142)$$

or, equivalently,

$$E_1 \equiv \{\mathbf{x} \mid \|\mathbf{y}\| \leq 1, \mathbf{y} \equiv \mathbf{L}_1^T(\mathbf{x} - \mathbf{c}_1)\}.$$

With the transformation

$$\mathbf{y} \equiv \mathbf{L}_1^T(\mathbf{x} - \mathbf{c}_1), \quad (143)$$

E_1 is transformed to the unit ball at the origin (denoted by E'_1) and E_2 is transformed to E'_2 , see Fig. 13. The point \mathbf{y}_2 in E'_2 which is closest to the origin is determined by the closest point algorithm (see Sec. 8). If $\|\mathbf{y}_2\|$ is less than unity, then E_1 and E_2 intersect.

For the case in which E_1 and E_2 do not intersect, we define

$$\mathbf{y}_1 = \mathbf{v} = \mathbf{y}_2 / \|\mathbf{y}_2\|, \quad (144)$$

so that \mathbf{y}_1 and \mathbf{y}_2 are the pair of closest points in E'_1 and E'_2 . Note that \mathbf{v} is a unit vector. Then we define

$$\mathbf{y}_h \equiv \frac{1}{2}(\mathbf{y}_1 + \mathbf{y}_2), \quad (145)$$

and a separating hyperplane is defined by

$$H' \equiv \{\mathbf{y} \mid \mathbf{v}^T(\mathbf{y} - \mathbf{y}_h) = 0\}. \quad (146)$$

Inverting the transformation Eq.(143), we obtain the separating hyperplane in the original space:

$$H \equiv \{\mathbf{x} \mid \mathbf{u}^T(\mathbf{x} - \mathbf{x}_h) = 0\}, \quad (147)$$

where

$$\mathbf{u} = \frac{\mathbf{L}_1 \mathbf{v}}{\|\mathbf{L}_1 \mathbf{v}\|}, \quad (148)$$

and

$$\mathbf{x}_h = \mathbf{c}_1 + \mathbf{L}_1^{-T} \mathbf{y}_h. \quad (149)$$

For a hyperplane H given by Eq.(147) (for some \mathbf{u} and \mathbf{x}_h), we define the quality q as follows. Let \mathbf{x}_1 be the point in E_1 closest to H , and similarly let \mathbf{x}_2 be the point in E_2 closest to H . The quality q is defined as

$$q \equiv \frac{\mathbf{u}^T(\mathbf{x}_2 - \mathbf{x}_1)}{|\mathbf{x}_2 - \mathbf{x}_1|} \leq 1. \quad (150)$$

This is the distance between the supporting hyperplanes at \mathbf{x}_1 and \mathbf{x}_2 relative to their separation. The maximum possible distance between the supporting hyperplanes is achieved for $q = 1$, and this occurs when \mathbf{x}_1 and \mathbf{x}_2 are the mutually closest points in E_1 and E_2 .

In the routine `ell_pair_separate` there is an option to iteratively improve the quality of the hyperplane. Initially \mathbf{x}_1 and \mathbf{x}_2 are set to the points in E_1 and E_2 corresponding to \mathbf{y}_1 and \mathbf{y}_2 (in E'_1 and E'_2). Then, successively, \mathbf{x}_1 is replaced by the closest point in E_1 to \mathbf{x}_2 ; and then \mathbf{x}_2 is replaced by the closest point in E_2 to \mathbf{x}_1 . The hyperplane is then taken as the perpendicular bisector of the line $\mathbf{x}_1 - \mathbf{x}_2$. It is not guaranteed that this hyperplane is separating, nor that the quality increases with the iterations, although it generally does. Consequently, H is taken as the hyperplane with the greatest quality encountered initially or during the iterations.

(Note that the separating hyperplane of quality $q = 1$ could alternatively be obtained by solving the quadratic programming problem, of determining the mutually closest points \mathbf{x}_1 and \mathbf{x}_2 in E_1 and E_2 . This has not been implemented.)

16 Pair covering query

Given a pair of ellipsoids E_1 and E_2 (centered at \mathbf{c}_1 and \mathbf{c}_2 and with Cholesky factors \mathbf{L}_1 and \mathbf{L}_2), the problem is to determine whether E_1 covers E_2 . This query is answered by the routine `ell_pair_cover_query` by the following algorithm.

With the same transformation as used in Sec. 15, E_1 is transformed to the unit ball, at the origin, and E_2 to E'_2 (see Eq.(143) and Fig.13). The algorithm described in Sec. 9 is then used to determine the distance s from the origin to the furthest point in E'_2 . The ellipsoid E_1 covers E_2 if and only if s is less than or equal to unity.

17 Shrink ellipsoid so that it is covered by a concentric ellipsoid

Given two concentric ellipsoids, E_1 , and E_2 , the task is to form the maximal-volume ellipsoid, E , which is covered by both E_1 and E_2 . This is performed by the routine `ell_pair_shrink`.

Clearly E is concentric with E_1 and E_2 , and so, without loss of generality, we take the origin at the mutual center. Then, E_1 is given by

$$E_1 \equiv \{\mathbf{x} \mid \|\mathbf{L}_1^T \mathbf{x}\| \leq 1\}, \quad (151)$$

and similarly for E_2 and E (in terms of \mathbf{L}_2 and \mathbf{L} , respectively).

The transformation

$$\mathbf{y} = \mathbf{L}_1^T \mathbf{x}, \quad (152)$$

maps E_1 to the unit ball, E'_1 , and it maps E_2 to the ellipsoid E'_2 with Cholesky factor

$$\mathbf{L}'_2 = \mathbf{L}_1^{-1} \mathbf{L}_2, \quad (153)$$

see Fig. 14. Note that E'_1 shares the principal axes of E'_2 . Hence E' (i.e., the mapped covered ellipsoid E) has the same principal directions as E'_2 ; and

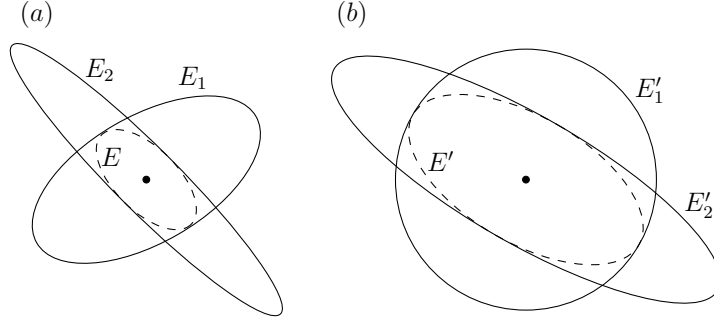


Figure 14: (a) Sketch of the concentric ellipsoids E_1 and E_2 and the maximal-volume ellipsoid E which is covered by them (b) Corresponding ellipsoids in the transformed space in which E'_1 is the unit ball.

the lengths of its principal axes are the lesser of those of E'_1 (all of which are unity) and those of E'_2 . Thus if

$$\mathbf{L}'_2 = \mathbf{U}\mathbf{\Sigma}\mathbf{V}^T, \quad (154)$$

is the SVD of \mathbf{L}'_2 , so that

$$\mathbf{L}'_2\mathbf{L}'_2{}^T = \mathbf{U}\mathbf{\Sigma}^2\mathbf{U}^T, \quad (155)$$

then the Cholesky matrix of E' is given by

$$\mathbf{L}'\mathbf{L}'^T = \mathbf{U}\tilde{\mathbf{\Sigma}}^2\mathbf{U}^T, \quad (156)$$

where the singular values $\tilde{\Sigma}_{ii} = \tilde{\sigma}_i$ are given by

$$\tilde{\sigma}_i = \max(\sigma_i, 1), \quad (157)$$

where $\sigma_i \equiv \Sigma_{ii}$.

The Cholesky matrix of E is obtained by inverting the transformation:

$$\mathbf{L} = \mathbf{L}_1\mathbf{L}'. \quad (158)$$

The same algorithm can be used to determine the minimal-volume ellipsoid which covers E_1 and E_2 . In that case, in contrast to Eq.(157), the appropriate singular values are:

$$\bar{\sigma}_i = \min(\sigma_i, 1). \quad (159)$$

18 Ellipsoid that covers two given ellipsoids

Given two ellipsoids E_1 and E_2 , the task is to determine a third ellipsoid E that covers both E_1 and E_2 . Ideally E is of minimal volume.

It is a problem of convex optimization to determine the minimum-volume covering ellipsoid (see, e.g., Boyd and Vandenberghe 2004). An algorithm is provided by Yildirim (2006). It appears that the solution to this convex optimization problem is computationally expensive. Instead, in the subsections, we describe heuristic algorithms with determine ellipsoids E (not of minimal volume) which cover E_1 and E_2 . These methods are implemented in the routine `ell_pair_cover`, with the parameter `algorithm` determining the particular algorithm to be used.

18.1 Spheroid algorithm

The ellipsoids E_1 and E_2 have centers \mathbf{c}_1 and \mathbf{c}_2 , and outer radii $r_{\text{out},1}$ and $r_{\text{out},2}$. Thus the ball B_1 centered at \mathbf{c}_1 of radius $r_{\text{out},1}$ covers E_1 , and similarly we define the ball B_2 which covers E_2 . In this “spheroid algorithm” (`algorithm` = 1) we take E to be the minimum-volume ball B which covers B_1 and B_2 .

The center and radius of B are determined as follows. Consider the line of centers with distance s measured from \mathbf{c}_1 towards \mathbf{c}_2 . Let the distance between the centers be $\Delta c \equiv |\mathbf{c}_2 - \mathbf{c}_1|$. There are four intersections between the ball B_1 and B_2 and the line. The outermost of these corresponds to

$$s_{\text{max}} = \max(r_{\text{out},1}, \Delta c + r_{\text{out},2}), \quad (160)$$

and

$$s_{\text{min}} = \min(-r_{\text{out},1}, \Delta c - r_{\text{out},2}). \quad (161)$$

Thus the center of B is

$$\mathbf{c} = \mathbf{c}_1 + \frac{1}{2}(s_{\text{min}} + s_{\text{max}})(\mathbf{c}_2 - \mathbf{c}_1)/\Delta c, \quad (162)$$

and its radius is

$$r = \frac{1}{2}(s_{\text{max}} - s_{\text{min}}). \quad (163)$$

A variant is the “spheroid algorithm with shrinking” (algorithm = 4), in which r is decreased to r' to yield the ball B' of minimum volume centered at \mathbf{c} which covers E_1 and E_2 . The radius r' is determined as the greatest distance from \mathbf{c} to any point in E_1 and E_2 (which is determined by `ell_pt_near_far`).

18.2 Covariance algorithm

The ellipsoid E_1 is defined by

$$E_1 \equiv \{\mathbf{x} \mid (\mathbf{x} - \mathbf{c}_1)^T \mathbf{A}_1 (\mathbf{x} - \mathbf{c}_1) \leq 1\}, \quad (164)$$

and E_2 and E are similarly defined by \mathbf{c}_2 and \mathbf{A}_2 , and by \mathbf{c} and \mathbf{A} , respectively.

In the “covariance” algorithm described in this section, we define the covering ellipsoid E by

$$\mathbf{c} \equiv \frac{1}{2}(\mathbf{c}_1 + \mathbf{c}_2), \quad (165)$$

$$\mathbf{A} \equiv \alpha \mathbf{A}_0, \quad (166)$$

and

$$\mathbf{A}_0 \equiv \left(\mathbf{A}_1^{-1} + \mathbf{A}_2^{-1} + \frac{1}{4}[\mathbf{c}_1 - \mathbf{c}_2][\mathbf{c}_1 - \mathbf{c}_2]^T \right)^{-1}, \quad (167)$$

where α is a positive parameter to be determined.

To determine α , we consider the ellipsoid E_0 defined by \mathbf{c} and \mathbf{A}_0 . With \mathbf{L}_0 being the Cholesky factor

$$\mathbf{L}_0 \mathbf{L}_0^T = \mathbf{A}_0, \quad (168)$$

we perform the linear transformation

$$\mathbf{y} = \mathbf{c} + \mathbf{L}_0^{-T} \mathbf{x}. \quad (169)$$

As depicted in Fig. 15, this transforms E_0 to the unit ball, and E_1 and E_2 to ellipsoids denoted by E'_1 and E'_2 .

Using the furthest-point algorithm (see Sec. 9), we determine \mathbf{y}_1 and \mathbf{y}_2 , defined as the points on E'_1 and E'_2 , respectively, which are furthest from the origin (see Fig. 15). Clearly, the ball E' of radius

$$r \equiv \max(\|\mathbf{y}_1\|, \|\mathbf{y}_2\|) \quad (170)$$

covers E'_1 and E'_2 . This corresponds to E' (the transformation of E) with

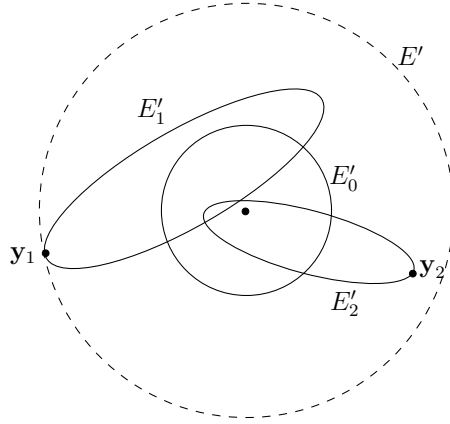


Figure 15: In the transformed space, the ellipsoid E'_0 which is the unit ball, the ellipsoids E'_1 and E'_2 , and the covering ellipsoid E' .

$$\alpha = r^{-2}. \quad (171)$$

In summary the ellipsoid E which covers E_1 and E_2 is defined by \mathbf{c} Eq.(165) and \mathbf{A} Eq.(166), where \mathbf{A}_0 and α are given by Eqs. (167), (170), and (171). The routine `ell_pair_cover` includes two implementations of this covariance algorithm. The first (`algorithm = 5`) is a direct implementation of the above equations in which \mathbf{A}_0 is formed and then \mathbf{L}_0 is obtained by Cholesky decomposition. The second implementation (`algorithm = 2`), now described, is preferred, since it avoids the formation of \mathbf{A}_0 , and hence is significantly more accurate.

With \mathbf{L}_1 and \mathbf{L}_2 being the Cholesky factors of \mathbf{A}_1 and \mathbf{A}_2 , and with $\mathbf{d} \equiv \frac{1}{2}(\mathbf{c}_1 - \mathbf{c}_2)$, we define the $(2n + 1) \times n$ matrix \mathbf{B} by

$$\mathbf{B}^T = [\mathbf{L}_1^{-T} \quad \mathbf{L}_2^{-T} \quad \mathbf{d}], \quad (172)$$

so that the inverse of Eq.(167) can be written

$$\mathbf{A}_0^{-1} = \mathbf{L}_0^{-T} \mathbf{L}_0^{-1} = \mathbf{B}^T \mathbf{B}. \quad (173)$$

Now let the QL factorization of \mathbf{B} be

$$\mathbf{B} = \mathbf{Q} \begin{bmatrix} 0 \\ \mathbf{L} \end{bmatrix}, \quad (174)$$

so that

$$\mathbf{B}^T \mathbf{B} = \mathbf{L}^T \mathbf{L}. \quad (175)$$

By comparing the above two equations, we see that \mathbf{L}_0 is the inverse of \mathbf{L} . Thus, in this preferred QL implementation of the covariance algorithm, the Cholesky matrix \mathbf{L}_0 required in Eq.(169) is obtained as \mathbf{L}^{-1} , where \mathbf{L} is obtained from the QL factorization of \mathbf{B} , defined by Eq.(172).

18.3 Iterative algorithm

The algorithm described here (which is also implemented in the routine `ell_pair_cover` with `algorithm= 2`), is more elaborate and expensive than the “covariance” algorithm described in the previous subsection, but in most circumstances it generates a covering ellipsoid E of smaller volume.

Given E_1 and E_2 , the algorithm proceeds through six stages (described below) to generate the covering ellipsoid E . Stages 1, 2 and 6 are trivial, but are retained for consistency with the implementation in `ell_pair_cover`. In Stages 3 and 4 the shape of E (but not its center and size) are determined. The center of E is taken to be on the line of centers of E_1 and E_2 . Its location is determined iteratively in Stage 5 so as to minimize the volume of E .

Various spaces are considered, and are referred to as \mathbf{x} -space, \mathbf{y} -space, \mathbf{z} -space and ζ -space. The ellipsoids E_1 and E_2 are given in \mathbf{x} -space, and the covering ellipsoid E is to be determined in this space. The other spaces are obtained by successive linear transformations; and $E_2(\mathbf{z})$, for example, denotes the ellipsoid E_2 viewed in \mathbf{z} -space, which has center $\mathbf{c}_2(\mathbf{z})$ and Cholesky triangle $\mathbf{L}_2(\mathbf{z})$.

18.3.1 Stage 1

The two ellipsoids E_1 and E_2 are given in \mathbf{x} -space (in terms of \mathbf{c}_1 , \mathbf{L}_1 , \mathbf{c}_2 and \mathbf{L}_2): see Fig.16(a).

18.3.2 Stage 2

We denote by E_1^0 and E_2^0 the two given ellipsoids shifted to the origin: see Fig.16(b). (In general, E_m^0 denotes E_m shifted to the origin.)

18.3.3 Stage 3

The transformed variable \mathbf{y} is defined by

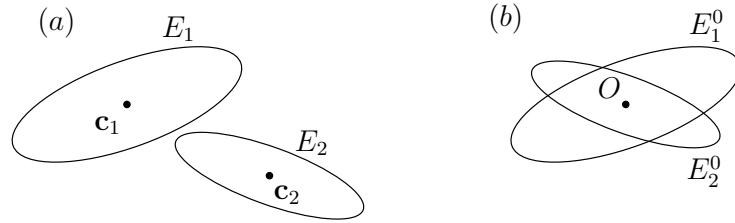


Figure 16: In \mathbf{x} -space, sketches of (a) the ellipsoids E_1 and E_2 in stage 1 (b) the ellipsoids E_1^0 and E_2^0 in stage 2.

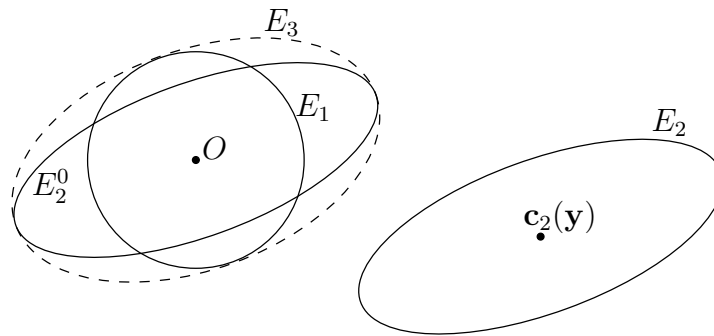


Figure 17: In \mathbf{y} -space, sketches of the various ellipsoids in stage 3.

$$\mathbf{y} \equiv \mathbf{L}_1^{-1}(\mathbf{x} - \mathbf{c}_1), \quad (176)$$

so that $E_1(\mathbf{y})$ is the unit ball at the origin.

At this stage a test is performed to determine if E_1 covers E_2 ; if it does, then $E = E_1$ is the minimal volume covering ellipsoid. Similarly, a test is performed to determine if E_2 covers E_1 . The way in which this testing is performed is described in Section 18.3.7. If neither E_1 nor E_2 covers the other, then the algorithm proceeds.

The ellipsoid E_3 is defined to be the minimal-volume ellipsoid which covers E_1^0 and E_2^0 (see Fig.17). This is readily determined: $E_3(\mathbf{y})$ has the same principal directions as E_2^0 , and the lengths of its principal semi-axes are the greater of those of $E_2^0(\mathbf{y})$ and $E_1^0(\mathbf{y})$ (which are unity).

18.3.4 Stage 4

A transformation (to \mathbf{z} -space) is performed which consists of a rotation such that the principal axes of E_1 , E_2 and E_3 are aligned with the coordinate

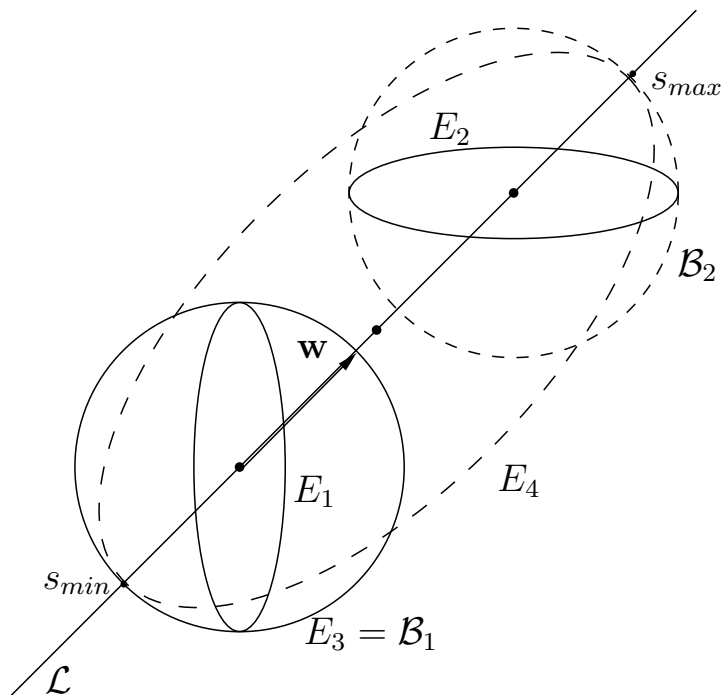


Figure 18: In \mathbf{z} -space, sketch of ellipsoids in stage 4 showing the construction of E_4 based on the extreme intersections (s_{\min} and s_{\max}) of the bounding balls \mathcal{B}_1 and \mathcal{B}_2 with the line of centers \mathcal{L} .

axes, followed by a stretching in the coordinate directions to make $E_3(\mathbf{z})$ the unit ball at the origin (see Fig.18). This transformation is readily determined from the SVD of $\mathbf{L}_2(\mathbf{y})$. Note that the principal semi-axes of $E_1(\mathbf{z})$ and $E_2(\mathbf{z})$ are aligned with the coordinate directions; their lengths are at most unity; and in each direction the length of the principal semi-axis of $E_1(\mathbf{z})$ and/or $E_2(\mathbf{z})$ equals unity. The line of centers \mathcal{L} between $E_1(\mathbf{z})$ and $E_2(\mathbf{z})$ can be written

$$\mathcal{L} \equiv \{\mathbf{z} \mid \mathbf{z} = \mathbf{w}s\},$$

where $\mathbf{w} = \mathbf{c}_2(\mathbf{z})/|\mathbf{c}_2(\mathbf{z})|$ is the unit vector from the origin to the center of $E_2(\mathbf{z})$, and s is the distance along the line.

Let \mathcal{B}_1 denote the bounding ball of $E_1(\mathbf{z})$. This is centered at the origin and has radius less than or equal to unity. There are two intersections of \mathcal{B}_1 and \mathcal{L} which occur at distances s_{1-} and s_{1+} along \mathcal{L} . Similarly the bounding ball \mathcal{B}_2 of $E_2(\mathbf{z})$ intersects \mathcal{L} at distances s_{2-} and s_{2+} . We define the extrema

of these intersections by

$$s_{\min} \equiv \min(s_{1-}, s_{1+}, s_{2-}, s_{2+}), \quad (177)$$

and

$$s_{\max} \equiv \max(s_{1-}, s_{1+}, s_{2-}, s_{2+}). \quad (178)$$

The ellipsoid E_4 is now defined to be centered at

$$s_0 \equiv \frac{1}{2}(s_{\min} + s_{\max}), \quad (179)$$

to have a principal semi-axis of length $\frac{1}{2}(s_{\max} - s_{\min})$ in the direction \mathbf{w} , and to have all other principal axes unity. In other words, $E_4(\mathbf{z})$ is formed from the unit ball at s_0 by stretching it in the $\pm\mathbf{w}$ directions so that it intersects the extrema s_{\min} and s_{\max} .

18.3.5 Stage 5

A transformation is performed to ζ -space such that $E_4(\zeta)$ is the unit ball at the origin, and the line of centers $\mathcal{L}(\zeta)$ is in the first coordinate direction:

$$\mathcal{L}(\zeta) = \{\zeta \mid \zeta_i = t\delta_{i1}\}, \quad (180)$$

where t measures the distance along the line (see Fig.19).

The covering ellipsoid being constructed $E(\zeta)$ is a ball of radius r_0 centered at a distance t_0 along \mathcal{L} . It remains to determine r_0 and t_0 .

Consider a ball centered at a distance t along \mathcal{L} . Let $r_1(t)$ denote the distance from the ball's center to the furthest point in $E_1(\zeta)$. This can be determined by the algorithm described in Section 9. Similarly, let $r_2(t)$ denote the distance to the furthest point in $E_2(\zeta)$; and we define

$$r(t) \equiv \max(r_1(t), r_2(t)). \quad (181)$$

Thus the ball centered at a distance t along \mathcal{L} and of radius $r(t)$ covers both $E_1(\zeta)$, and $E_2(\zeta)$.

In the definition of $E(\zeta)$, we take t_0 to be (an approximation to) the value of t at which $r(t)$ is minimum, and then define $r_0 \equiv r(t_0)$

As one moves along the line \mathcal{L} from the center of $E_1(\zeta)$ to the center of $E_2(\zeta)$, $r_1(t)$ continually increases and $r_2(t)$ continually decreases. Except in unusual circumstances, the minimum of $r(t)$ occurs between the centers, where $r_1(t)$ equals $r_2(t)$. A simple iterative procedure usually determines the location of the minimum (to reasonable accuracy) in two or three iterations.

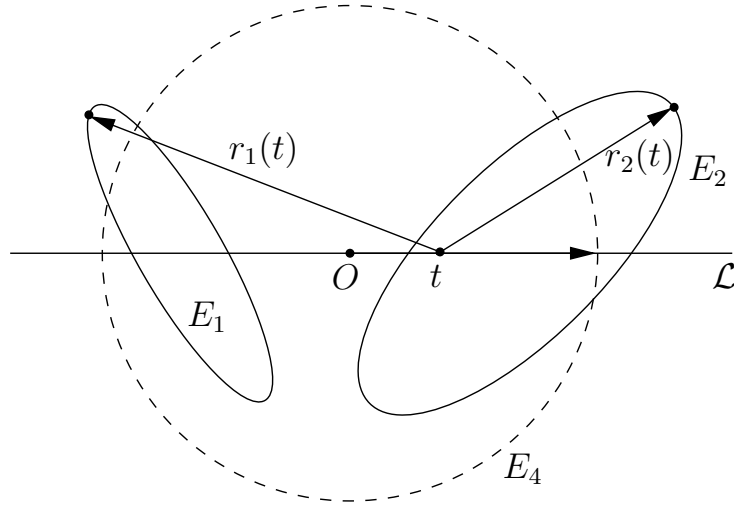


Figure 19: In ζ -space, sketch showing ellipsoids in stage 5, the general point t on the line of centers \mathcal{L} , and the distances $r_1(t)$ and $r_1(t)$ to the furthest points in E_1 and E_2 , respectively.

18.3.6 Stage 6

The covering ellipsoid $E(\zeta)$ obtained in Stage 5 is transformed to the original coordinate system to yield the required ellipsoid $E(\mathbf{x})$ which covers E_1 and E_2 .

18.3.7 Mutual covering

In Stage 3 it is required to determine if $E_1(\mathbf{y})$ covers $E_2(\mathbf{y})$ and *vice versa*. The procedure used is now described.

Let ρ be the distance from the origin to the furthest point in $E_2(\mathbf{y})$. Since $E_1(\mathbf{y})$ is the unit ball at the origin, E_1 covers E_2 if, and only if, ρ is less than or equal to unity.

While ρ can be evaluated using the algorithm described in Section 9, this involves quadratic minimization and hence is somewhat expensive. As now described, there are easily computed bounds on ρ so that its exact evaluation can often be avoided.

Let d be the distance between the centers of $E_1(\mathbf{y})$ and $E_2(\mathbf{y})$, and let $r_{2,\min}$ and $r_{2,\max}$ be the lengths of the smallest and largest principal semi-axes of $E_2(\mathbf{y})$. From the triangle inequality we then have

$$\rho \leq d + r_{2,\max}, \quad (182)$$

and

$$\rho \geq d + r_{2,\min}. \quad (183)$$

We also have

$$\rho \geq r_{2,\max}. \quad (184)$$

Thus, if $d + r_{2,\max} \leq 1$, then $\rho \leq 1$, and so E_1 covers E_2 . On the other hand, if $d + r_{2,\min} > 1$ or $r_{2,\max} > 1$, then $\rho > 1$, and so E_1 does not cover E_2 . In the remaining cases, E_1 may cover E_2 , and so ρ is evaluated.

18.3.8 Discussion

While this algorithm is more elaborate and expensive than that given in Section 18.2, it generally yields a covering ellipsoid E of smaller volume. In particular it yields the ellipsoid of minimal volume if E_1 and E_2 are concentric or if one covers the other.

The principal computational expenses are:

1. The SVD of $\mathbf{L}_2(\mathbf{y})$ performed in Stage 3
2. The quadratic minimization involved in the furthest-point algorithm (Section 9) which is invoked 0, 1 or 2 times (in Stage 3) to determine if E_1 and E_2 cover each other
3. The quadratic minimization involved in the furthest-point algorithm which is invoked twice per iteration (to evaluate $r_1(t)$ and $r_2(t)$) in Stage 5.

19 Conclusions

Algorithms have been described for performing some basic geometric operations on ellipsoids. A Fortran implementation of these algorithms is provided by the Ell.LIB library.

20 Acknowledgments

I am particularly grateful to Professor Charles Van Loan for his help on numerous occasions with issues of numerical linear algebra.

References

- Averick, B. M., R. Carter, and J. More (1993). MINPACK-2. <http://www-fp.mcs.anl.gov/OTC/minpack/summary.html>.
- Boyd, S. and L. Vandenberghe (2004). *Convex Optimization*. Cambridge: Cambridge University Press.
- Golub, G. H. and C. F. Van Loan (1996). *Matrix Computations* (3rd ed.). Baltimore: Johns Hopkins University Press.
- Pope, S. B. (1997). Computationally efficient implementation of combustion chemistry using *in situ* adaptive tabulation. *Combust. Theory Modelling 1*, 41–63.
- Yildirim, E. A. (2006). On the minimum volume covering ellipsoid of ellipsoids. *SIAM Journal on Optimization 17*, 621–641.